Journal of the Energy Institute 116 (2024) 101762

Contents lists available at ScienceDirect

Journal of the Energy Institute

journal homepage: www.elsevier.com/locate/joei

A review of CO emissions during solid biofuel combustion – Formation mechanisms and fuel-related reduction measures

Theresa Siegmund [*], Christian Gollmer, Marvin Scherzinger, Martin Kaltschmitt

Institute of Environmental Technology and Energy Economics, Hamburg University of Technology (TUHH), Eissendorfer Strasse 40, 21073, Hamburg, Germany

ARTICLE INFO

Handling Editor: Dr. Paul Williams

Keywords:
Carbon monoxide (CO)
Biomass combustion
Emissions
Fuel measures
Potassium
Additivation

ABSTRACT

Minimizing carbon monoxide (CO) emissions from the combustion of solid biofuels is essential to improve thermo-chemical conversion efficiencies and avoid impact on human health. This review focuses on the formation mechanisms and subsequent oxidation of CO within the combustion process; for this, the different phases of biomass combustion (i.e., heating up, pyrolysis, gasification, and homogeneous gas-phase oxidation) are considered separately. The comprehensive analysis shows that CO emissions can be mitigated by fuel-related measures (e.g., washing and leaching to eliminate K components) as well as by (mineral) additivation of the fuel to repress the K-release by binding it in temperature-stable components within the ash. Furthermore, the addition of sulfur results in the sulfation of critical K-compounds to less corrosive and non-radical interfering compounds.

1. Introduction

Solid biomass currently contributes with more than 65 % to the overall use of renewable sources of energy within the German heating sector [1]. Biomass utilization is and will most likely remain an essential component for decentralized energy systems/local heat provision, even though general acceptance of using wood as a fuel has decreased at least in Germany [2]. Simultaneously, incentives (i.e., mainly subsidies) for biomass deployment in the heating sector are available in many European countries [3]. For instance, in Germany, federal funding for efficient buildings (BEG) supports households in switching to eco-friendly heating, including biomass heating systems. Here, additional bonuses are provided when total particulate matter (TPM) emission limits of 2.5 mg/m^3 are met [4]. Energy derived from solid biofuels undoubtedly has some advantages; for instance, it can be used with existing technology and is well-known in rural areas [5]. Additionally, the use of solid biomass combustion is generally considered a carbon neutral/low-carbon. Nevertheless, there is a tradeoff between these gains, air pollution and associated health issues (e.g., due to the release of organic gaseous compounds (OGC), or the formation of carbon monoxide (CO), particulate matter (PM), and NO$_x$ during the thermo-chemical conversion of solid biofuels). To avoid or at least minimize such negative aspects, next to technical approaches for improving the combustion processes, the focus in research is often on the mitigation of TPM emissions (e.g., Refs. [6–12]). The reduction potential for CO emissions from lignocellulosic biomass on the other hand is neither fully understood nor fully explored. Still, legally defined threshold values for these emissions are in place, and at least for Germany, it can be expected that these legal limits will be more strict in the time to come [13]. In addition to the regulatory framework, the reduction in CO emissions is essential due to its toxicity and its impact on human health; also reducing CO emissions or promoting a higher degree of CO oxidation will improve combustion efficiencies and the overall performance of combustion units.

The efficiency and formation of pollutants during the combustion of biomass depends on the fuel composition and properties, as well as on the combustion unit itself. Various measures can be considered to reduce CO and other emissions, generally categorized into fuel-related, primary, and secondary measures. Table 1 provides examples of these measures and their CO mitigation potentials.

- Fuel-related measures address the fuel itself to allow for low CO emissions during combustion. This includes adjusting factors such as water content, chemical composition (e.g., through leaching), fuel particle size, fines content, or the addition of (mineral) components. The effort and additional cost for these measures vary depending on market prices (e.g., for the additives) and/or the energy intensity of the measure (e.g., for drying or milling.) Fuel-related measures can

---

[*] Corresponding author.
E-mail address: theresa.siegmund@tuhh.de (T. Siegmund).

https://doi.org/10.1016/j.joei.2024.101762
Received 6 February 2024; Received in revised form 23 July 2024; Accepted 24 July 2024
Available online 25 July 2024

Table 1

Examples of fuel-related, primary, and secondary measures and their effects on CO emissions during biofuel combustion. Unless otherwise specified, the first number in the “Values” column is the reference for the respective CO mitigation effects.

Measure		Values	Fuel	Furnace	CO mitigation	Reference
Fuel-related measures	Pellet length	10.3, 15.5, and 17.0 mm	Wood pellets	6 kW stove	Decrease in CO emissions of 25 and 38 % for medium and long pellets, respectively	[27]
				15 kW boiler	No effect for medium pellets, 50 % rise for long pellets	[27]
	Moisture content	3.3, 6.8, and 10.2 wt%	Wood pellets	6 kW stove	For 6.8 and 10.2 wt% a decrease of 47 % and 46 %, respectively	[27]
		9, 14, 19, and 25 wt%	Wood chips	83 kW boiler	Decrease of 13 %, 9 %, and a rise of 46 % for a moisture content of 25 wt%	[28]
	Fines content	0.1, 3, and 10 wt%	Wood pellets	6 kW stove	Rise in CO emissions of 132 % and 354 % for the higher fines contents, respectively	[27]
	Washing	6 h with deionized water	Fir, beech, and oak pellets	1.3–6.3 kW stove	Decrease of 32, 24, and 48 % for unwashed wood compared to washed wood, respectively	[29]
	Additivation	0.2 and 2.0 wt% kaolin	Spruce/willow mixture	12 kW boiler	54 % and 67 % decrease for pellets with additive compared to unadditivated pellets	[8]
		0.5 wt% kaolin and kaolinite	Wood chips	33 kW boiler	Decrease of 56–70 % for kaolin and 72 % for kaolinite	[9]
	Oxygen carrier aided combustion	Ilmenite as bed material	Biomass (unspecified)	19 MW bubbling fluidized bed	50 % CO reduction during the first day of operation with ilmenite in the bed	[30]
Primary measures	Primary air mass flow	0.03–0.6 kg/m^2s	Simulated waste	Fixed bed reactor ($l = 1.5$ m, $d = 200$ mm)	Decrease of up to 87 %	[14]
	Air-staging	–	Wood pellets	15 kW fixed bed reactor	50 % reduction of CO emissions compared to non-staged air supply	[31]
Secondary measures	Catalysts	Platinum (Pt) and palladium (Pd) as a pack of nets	Wood logs	18 kW stove	Average decrease of 26 % with catalysts	[32]
		Pt, Pd, and cerium (Ce) on cordierite and metal structure		13 kW fireplace	Decrease of 65–70 %. With heating system of fume: decrease of 80 % and 90 % during ignition and low-charge phase, respectively	[26]

be particularly advantageous for small-scale combustion units due to their low capital costs in contrast to secondary measures and offer additional reduction potential when primary measures reach their mitigation limits.

- Primary measures focus on improving the combustion process by adopting more efficient combustion technologies (e.g., optimizing combustion unit geometry, insulation, heat exchangers, and draught control [14–18]). Moreover, parameters like air staging, fuel load, and air-fuel ratio λ have an impact on the CO content within the flue gas [15,19].
- Secondary measures for CO emission reduction may sometimes be combined with the reduction of other airborne emissions like OGC, TPM, and NO_x [20]. These measures involve flue gas treatment, such as catalytic downstream conversion processes, mostly with precious metals [21–25]. Here, CO conversion efficiencies of up to 100 % can be achieved [21]. Since secondary measures handle only the flue gas, they offer flexible implementation, though electric heating of the flue gas might be necessary in order to reach the high temperatures required by the catalysts [26].

Over the past years, various measures beyond conventional approaches for emissions reduction and combustion enhancement have been studied in fixed bed combustion as well as fluidized bed systems. The methods range from co-combustion with other fuels [16,33,34], pre-treatment of the feedstock to reduce the content of certain elements (e.g., K, Na, Si, Mg, Ca through washing/leaching with acid and water [12,29,35–38]) or the pre-treatment with alkali metals for catalytic combustion [39–41]. Other approaches include adding gaseous and solid/mineral compounds to bind specific elements within the gas phase or from into the ash [8–11]. An additional motivation for adding minerals in combustion processes is their capacity to function as oxygen carriers [33–39]. Many of these measures have also been reported to reduce CO emissions; however, the mechanism behind these observations is often unclear.

Against this background, the aim of this review is the assembly of fragmented knowledge of isolated processes relevant to the formation and subsequent complete oxidation of CO during the combustion of solid biofuels. The objective is to bridge the gap between understanding individual mechanisms and their collective impact on lignocellulosic biomass combustion, thereby exploring holistic optimization possibilities. Within this context, the origin of CO emissions in lignocellulosic biomass combustion, starting from the pyrolytic degradation processes (section 2.1), the discussion of governing mechanisms and limitations in heterogenous solid-gas reaction and char oxidation (section 2.2), as well as homogenous gas-phase reactions of the released chemical compounds and CO oxidation (section 2.3) will be discussed. In addition, the influence of different combustion-related parameters (i.e., p, T, O_2, H_2O, CO_2, and hydrocarbons in section 3), as well as inorganic elements contained naturally in lignocellulosic biomass will be depicted (section 3.3). Subsequently, this background information is transferred to analyzing fuel-related and primary measures for CO emission reduction in combustion processes (section 4).

2. CO emissions during solid biofuel combustion

In order to gain a clear understanding of the governing mechanisms of CO release and oxidation during the combustion of lignocellulosic biomass, the overall decomposition behavior of the solid biofuel must first be understood. This thermo-chemical decomposition of solid biofuels can be divided into four phases, in each of which different intermediates are formed (Fig. 1). During the complete thermo-chemical conversion, these phases can occur sequentially and/or partly in parallel.

- The first combustion phase consists of the heating-up phase. Free and cell-bound water is released into the gas-phase surrounding the solid fuel particle.
- This is followed by a phase called pyrolytic degradation (air-fuel ratio $\lambda \approx 0$, endothermic), where the macromolecules the solid biofuel consists of (i.e., lignin, cellulose, hemicellulose) are broken down. The resulting fragments (e.g., CO, hydrocarbons C_nH_m, oxygenated hydrocarbons $C_xH_yO_z$) are released from the solid

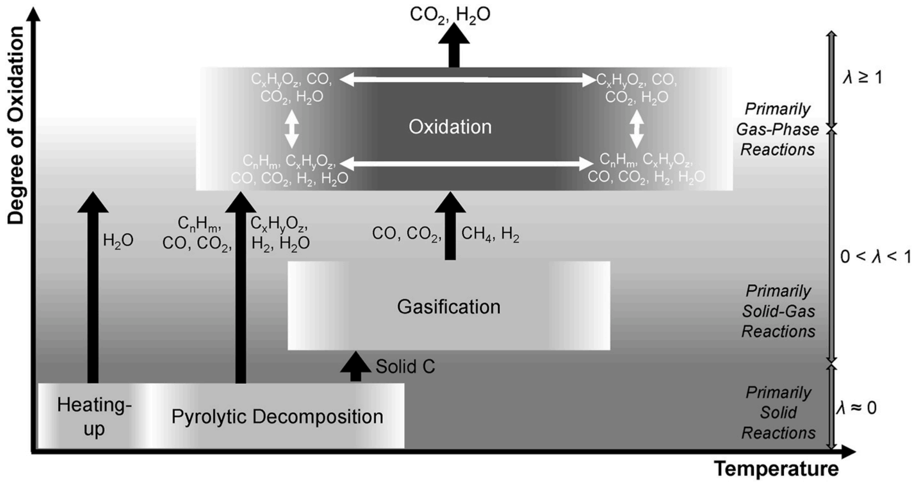

Fig. 1. Simplified phases of thermo-chemical conversion of solid biomass ($C_xH_yO_z$) with essential intermediate products. The boxes represent conversion phases (light: predominantly endothermic, dark: primarily exothermic). Adjusted from [19].

biomass/the fuel particle into the ambient gas-phase, creating a boundary layer around the fuel particle hindering reactions with the surrounding proximate gas-phase/combustion air, leaving behind (pyrolysis) char. Char (coal) is inevitably formed since lignocellulosic materials naturally have higher carbon contents relative to their oxygen and hydrogen content, preventing the complete transformation of the carbon into the gas phase during this pyrolytic decomposition phase.

- The subsequent phase for the remaining solid (char) is called gasification ($0 < \lambda < 1$). Here, the solid carbon (i.e., char/coke) is transferred from a solid into a gas (i.e., CO, CO_2, H_2, and CH_4). Therefore, oxygen or another oxidizing agent (e.g., H_2O, CO_2, H_2) is mandatory.
- Under (over)stoichiometric conditions, the remaining, not fully oxidized gas compounds and previously formed intermediate products coming from the two previous phases are then fully oxidized within this final phase called oxidation ($\lambda \geq 1$, exothermic) [19]. Due to thermodynamic and chemical reasons, the oxidation of these intermediates does not necessarily occur directly. Larger molecules, e.g., released during the pyrolytic decomposition phase, are fragmented into smaller molecules and further cracked and or oxidized within exothermal processes. This may be heat-induced, through (partial) oxidation and/or secondary gas-phase oxidation of gaseous and/or liquid products (e.g., CO, C_nH_m, $C_xH_yO_z$)),

CO emissions are typically the result of incomplete carbon oxidation. Related to solid biofuels, they can originate from either the pyrolytic decomposition of the lignocellulosic biomass, from the gasification of the char, and/or from secondary gas-phase reactions of the decomposition/conversion products. Accordingly, CO is formed in different phases during the thermo-chemical conversion of solid biofuels.

2.1. Phase "pyrolytic decomposition" (Solid reactions)

Lignocellulosic biomass, respectively solid biofuels, consist mainly of the three biopolymers cellulose, hemicellulose, and lignin (i.e., these biopolymers account for a share of 40–45 wt%, 20 to 35 wt%, and 15 to 30 wt% of dry wood, respectively) [19]. Due to the different structures and compositions of cellulose, hemicellulose, and lignin, the heat-induced decomposition of those components occurs within different temperature ranges.

- Cellulose has the largest macromolecule share within wood and herbaceous biomass and consists of linear and unbranched chains through β 1–4 D-glycosidic bonds.
- Hemicellulose comprises different monomer units, forming branched polysaccharides that serve multiple functions in the biogenic material.
- Lignin is a three-dimensional cross-linked aromatic polymer formed by units of alkylbenzenes and serves as a filler in biomass [19,42].

The decomposition of these polymers can be linked to their thermal stability (i.e., hemicellulose < cellulose < lignin). The decomposition temperatures are at approx. 220–320 °C for hemicellulose, 320–400 °C for cellulose, and the widest temperature range for lignin from 160-900 °C [43–45]. During the thermo-chemical decomposition of these biopolymers, volatile gases (e.g., CO, C_nH_m, $C_xH_yO_z$), condensable gases (e.g., C_nH_m, $C_xH_yO_z$), and liquid tars (e.g., C_nH_m, $C_xH_yO_z$) are formed, released by the solid biomass at sufficiently high temperatures into the surrounding gas atmosphere. Assuming thermally thin particles for uniform reaction temperatures and neglecting secondary reactions leading to further heat-induced cracked products (e.g., C_nH_m, $C_xH_yO_z$), the release of these volatiles from the solid biomass follows first-order Arrhenius kinetics [46].

CO_2 release is caused mainly by cracking, reforming, or cleavage of carbonyl (-C=O), carboxyl (-COOH), acetyl (-$COCH_3$), and ester (-COOR) functional groups being part of hemicellulose, cellulose and side chains of lignin. CO is mainly produced by cracking and reforming of ether bonds (C–O–C) and carbonyl groups (-C=O) [44] and from cleavage of –COOH and formyl (-CHO) radicals/fragments [47,48].

The characteristics of hemicellulose, cellulose, and lignin pyrolysis can be investigated with a thermogravimetric analyzer (TGA) and differential thermogravimetric analysis (DTG) while measuring the released gases using Fourier transform infrared (FTIR) spectroscopy (e.g., Refs. [43,44]). According to TGA results [47], CO_2 released during biomass pyrolysis can be mainly attributed to hemicellulose at temperatures below 500 °C and lignin at higher temperatures related to the realized experimental conditions. Looking at the release of CO [47], the yield can again be attributed to hemicellulose at relatively low temperatures (<600 °C) and high peaks of CO above 700 °C to lignin, presumably evolved from secondary pyrolysis of tar residues in the solid sample. Here, pyrolysis of cellulose contributed only to a small part to the release of CO and CO_2, while for fixed bed combustion, they obtained the highest CO yield for cellulose. This also agrees with the published results [35,41,42], suggesting hemicellulose and cellulose as the origin of CO and CO_2 release at lower temperatures.

Su et al. [49] studied the degradation behavior, the carbon oxide (i.e., CO and CO_2) production, and the heat properties of wood pyrolysis within different oxygen concentrations. Mass loss ranges in the TGA for inert atmospheres can be divided into dehydration, devolatilization or pyrolytic decomposition, and carbonization. In oxidative environments, the mass loss ranges in the TGA can be defined as dehydration, pyrolytic decomposition, and char oxidation (i.e., gasification and subsequent oxidation) (Fig. 2). Besides differences in mass loss, temperature intervals are also shifted forward with increasing oxygen content. That is due to different reasons: oxygen overcomes the diffusion resistances in the boundary layer resulting from the efflux of volatiles to reach and eventually react with the surface of the char/coke of the pyrolyzed fuel particle. This exothermic reaction then leads to an increase in surface temperature and further biomass decomposition. Another reason for promoted pyrolytic decomposition due to higher oxygen content is the increased oxyradical concentration, such as hydroxyl (${}^{\bullet}OH$) or peroxy radicals ($ROO^{\bullet}$) in the gaseous phase [49].

The above findings all result from batch decomposition experiments with defined temperature profiles. In real-world combustion processes, the phases of thermo-chemical conversion cannot be strictly separated since the temperature levels after the heating-up phase are typically at a level of 800 to 1000 °C in the core of the combustion zone of the respective combustion unit; outside this core, there might be a lower temperature level. This situation will lead to different decomposition behaviors, complex and overlapping reaction mechanisms, and thus a different product distribution visible within the gas phase [50]. In order to understand those mechanisms, reactive force fields (ReaxFF) have been used during molecular dynamics (MD) simulations. Reactive force fields (ReaxFF) are bond-order-dependent force fields providing insight into bond breaking and formation, allowing the investigation of complex reactions and molecular dynamics (MD) simulations (e.g., in large hydrocarbon (C_{100+}) systems over long time scales (i.e., hundreds of picoseconds)) [51]. While simulated temperature levels are often elevated well beyond those encountered in actual combustion processes (e.g., 1750 to 4000 °C) to expedite computational efforts, these simulations can offer insights into the formation mechanisms, pathways, and influential parameters governing CO emissions. In literature, the simulations performed revolve around either hydrocarbon systems [51,52], pyrolysis and/or combustion or gasification of cellulose [48,53], lignite or hard coal [54–57], and less often around lignocellulosic biomass [47,58].

By investigating the pyrolysis mechanism of wheat straw using reactive force fields (ReaxFF) with molecular dynamics (MD) simulations, it has been found that high temperatures result in higher gas and tar species generation rates [47]. The primary sources for the production of CO and CO_2 were cellulose and hemicellulose, with slightly more CO from cellulose and more CO_2 from hemicellulose due to the presence of more carboxyl and carbonyl groups. This also aligns with the results described above. CO and CO_2 were mainly produced from the cleavage of ${}^{\bullet}CHO_2$ radicals.

Chen et al. [58] conducted a model of the combustion process of biomass under various conditions, including different temperatures, oxidative levels, and humidity. Among other things, they observed increasing biomass decomposition in fuel-lean conditions and facilitated CO release at higher temperatures. In Ref. [48], the CO release mechanism in cellulose combustion was investigated using reactive force fields (ReaxFF). Based on dissociation energies and equilibrium bond distances, C–O bonds in cellulose are less thermally stable than C–C bonds. Cellulose was initially decomposed into smaller molecules such as $C_2H_2O_2$, C_2H_2O, CH_2O_2, and CH_2O, leading to the formation of the main free radicals ${}^{\bullet}CHO_2$ and ${}^{\bullet}CHO$, influencing the concentration of CO. Also, the decomposition of cellulose was significantly influenced by free ${}^{\bullet}OH$ radicals.

2.2. *Phase "gasification" (Heterogenous solid-gas reactions)*

When lignocellulosic biomass devolatilization reaches the final stages, gasification of the remaining solid char/coke, consisting mainly of carbon (C), occurs; i.e., the solid carbon is transferred into the gas phase with the help of a gaseous gasification agent (e.g., oxygen from ambient air). Thus, necessary heterogenous reactions are usually slower than homogenous reactions and depend strongly on the particle surface area. They can be limited by external and internal diffusion, convection of the oxidant to the particle, or reaction kinetics. At a temperature level where the gasification phase is typically realized, the former usually is the case, while at lower temperature levels with enough oxidant, the reaction kinetic determines the reaction progress.

Char gasification typically accounts for 20 % of the total weight loss from the biomass in combustion (volatile release accounts for 80 %), but high gross calorific values compensate for the smaller fuel consumption. Such char gasification primarily yields CO and CO_2; however, the gasification temperature of char is typically lower (<800 °C) than the necessary temperature level for complete CO oxidation [15]. The respective reaction mechanisms and selected influencing factors of such char gasification are given below (e.g., Ref. [59]).

Biomass char is heterogeneously bound to heteroatoms (e.g., H, O, N, S) influencing combustion properties; especially inorganic elements (i.e., d-block elements as well as alkali and alkaline earth metals) might have catalytic effects on carbon gasification. This biomass char is oxidized by O_2, CO_2, and H_2O as expressed in the reaction equation (1) - (4) [59–61].

$$C\ (s) + O_2 \leftrightharpoons CO_2 \tag{1}$$

$$2C\ (s) + O_2 \leftrightharpoons 2CO \tag{2}$$

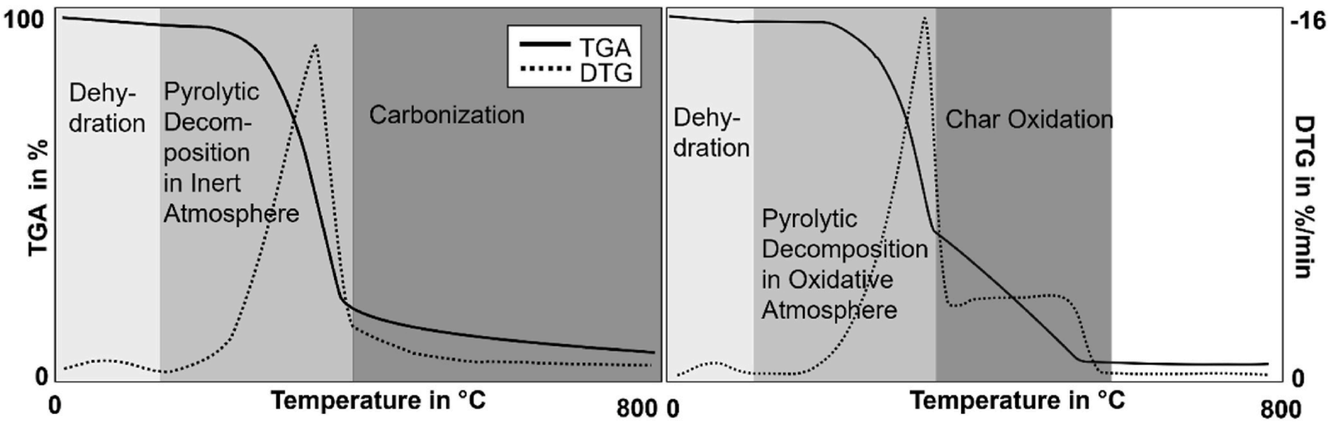

Fig. 2. Examples of TGA and DTG profiles and reaction phases of pyrolysis in inert (left) and oxidative (right) atmosphere. Adjusted from Ref. [49] for pine wood.

$$\mathrm{C\ (s) + CO_2 \leftrightharpoons 2CO} \quad (3)$$

$$\mathrm{C\ (s) + H_2O \leftrightharpoons CO + H_2} \quad (4)$$

Reaction enthalpies ΔH^0 and standard Gibb's energies ΔG^0 over a wide temperature range of equations (1) and (2) are negative, meaning the reactions are exothermic and thus favored. The Boudouard reaction (3) is endothermic (as is the water-gas reaction (4)) and becomes thus only relevant for temperature ranges above 700 °C [59].

Unlike homogenous reaction kinetics, transport phenomena often limit heterogenous solid-gas reactions/char combustion. Depending on the concentration of the locally available oxidant, overall reaction kinetics might differ from intrinsic reaction kinetics depending on temperature; further macroscopic insights into transport phenomena in the bulk phase and boundary layers, along with their dependence on particle pore structure, can be found, e.g., in Refs. [59,62].

- For relatively low gasification temperatures (<600 °C), char gasification reactions are slow. Under these circumstances, sufficient oxygen will be transported to the particle surface, and diffusion limitations can be neglected.
- In regimes with higher temperatures, reaction kinetics and thus oxygen consumption increase; transport mechanisms and oxidant diffusion become more relevant. For temperatures above 1000 °C, diffusion dominates [62]. This dependency can be expressed using parameters such as the effectiveness factor (η) and Thiele modulus (ϕ) in chemical reaction kinetics.
    - o For $\phi \ll 1$ and $\eta = 1$, the reaction is dominated by the intrinsic reaction rate (kinetic regime).
    - o For $\phi \gg 1$, the effectiveness factor is expressed as $\eta = 1/\phi$, and diffusion limitations must be accounted for [63].

Fig. 3 shows the fundamental steps of carbon/char gasification; oxygen diffuses toward the char surface through the bulk phase and boundary layers, allowing the adsorption of dioxygen molecules and oxygen atoms on active surface sites (e.g., defects, edges, dislocations, inorganic impurities, oxygen, hydrogen functional groups) [61]. Subsequently, dioxygen is split and reacts with the carbon surface atoms, leading to the primary formation of CO and CO_2 desorbing from the surface and diffusing back through the boundary layer.

When investigating the mechanisms behind CO and CO_2 formation during char/coke gasification, the Langmuir-Hinshelwood model becomes pertinent, describing the adsorption and desorption processes relevant to oxidation. This model involves the adsorption of O_2 onto the particle surface and the desorption of CO and CO_2. This ad- and desorption can occur through single or dual side mechanisms, necessitating one or two adjacent free carbon sites [61].

The understanding of CO formation mechanisms in char gasification with O_2 requires extending the reactions according to equation (1) - (4) to include intermediate adsorbed species like C(O) and active and available carbon sites C_f. The extended mechanisms for char oxidation with O_2 and CO_2 are depicted in equation (5) - (9) [60,62,64]. The reaction (9) is reported to be much slower than the former reactions (5) - (8).

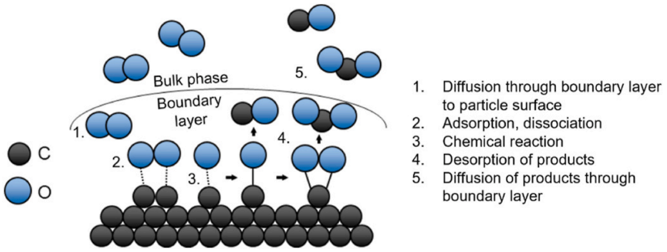

Fig. 3. Steps of carbon oxidation reactions (partly according to Ref. [59]).

$$\mathrm{2C_f + O_2 \leftrightharpoons 2C(O)} \quad (5)$$

$$\mathrm{C(O) \rightarrow CO} \quad (6)$$

$$\mathrm{2C(O) \leftrightharpoons CO_2 + C}_f \quad (7)$$

$$\mathrm{3C(O) + O_2 \ \rightarrow \ 2CO_2 + C(O)} \quad (8)$$

$$\mathrm{C_f + CO_2 \leftrightharpoons CO + C(O)} \quad (9)$$

Considering the influence of inorganic metals on char gasification, their effect on reaction (9) (e.g., acceleration by K) is expressed in reactions (10) and (11), followed by CO desorption (reaction (6)). Available metal sites are represented by "*" [60].

$$* + \mathrm{CO_2 \leftrightharpoons CO + O}* \quad (10)$$

$$\mathrm{O}* + \mathrm{C_f \leftrightharpoons C(O)} + * \quad (11)$$

Similar reaction pathways can be formulated for O_2, H_2, and H_2O [60]. The C(O) complexes serve as oxygen reservoirs, building surface oxide complexes that might be mobile but not always reactive. This indicates that not all chemisorbed oxygen species may react; some complexes may be mobile yet unable to desorb [59].

The presence of CO also has inhibiting effects on the C(O) complexes [64]. Generally, CO_2 generation is prominent at lower temperatures, whereas CO gains significance at elevated temperatures, reduced pressures, and typically under conditions of low oxygen availability. This may be attributed to different reasons, including surface chemistry, factors like sequential series of reactions related to lactone formation [59], or the favored formation of CO_2 on inorganic sites and heightened catalytic performance at lower temperatures. In contrast to this, CO formation occurs at carbon edges, which is favored at higher temperatures [61].

2.3. *Phase "oxidation" (Homogenous gas-phase reactions)*

The gases released from the solid biomass during the phase of pyrolytic degradation make up for 80 % of the total weight loss of lignocellulosic biomass. The released large macromolecules are broken down into smaller components, including condensable gases such as acetic acid, aromatic compounds, phenolic derivates, and aldehydes or non-condensable gases such as CH_4, CO_2, H_2, CO, volatiles (summarized as $C_xH_yO_z$) and other hydrocarbons (C_nH_m) [42]. While the oxidation of volatiles leads to flaming combustion in the gas-phase, char oxidation typically occurs as smoldering [65].

Most of the released heat in combustion is attributed to exothermic gas-phase oxidation reactions [66]. The main gaseous components present in the gas phase, where the oxidation phase takes place, include CO, CO_2, H_2O, CH_4, and other hydrocarbons that are volatile under these temperature conditions [31]. In the presence of an oxidizing agent (i.e., ambient air/oxygen), previously emitted hydrocarbons and other volatiles can be rapidly oxidized to CO_2 and H_2O. The start of the respective oxidation reactions requires ignition with a spark, flame, or self-ignition at sufficiently elevated temperatures [65]. Self-ignition temperatures for hydrocarbons vary in the range of approx. 530–630 °C, 230–280 °C, and 340–500 °C for CH_4, H_2 and CO, respectively [67]. In stable flaming, the combustion occurs directly in the gas phase outside the solid phase [65].

Equilibrium compositions in the gas phase of such combustion/oxidation processes can be easily calculated. However, since equilibrium conditions in such (fast) homogenous gas phase oxidation reactions are usually not reached due to short residence times, reaction kinetics have to be considered [15]. In this context, the oxidation of volatile compounds ($C_xH_yO_z$) can be expressed according to equation (12), with f being a dimensionless factor between 0 and 1 ($f = 0$ and $f = 1$ promoting only CO and CO_2 formation, respectively). This factor is linked to the specific oxidation conditions and parameters, including temperature, pressure, and the system composition (i.e., fuel and gas phase composition) [19,46,59].

$$C_xH_yO_z + \left(\frac{x}{2}(f+1) + \frac{y}{4} - \frac{z}{2}\right)O_2 \rightarrow x(1\text{-}f)CO + xfCO_2 + \frac{y}{2}H_2O \tag{12}$$

Several approaches for kinetic mechanisms of gas-phase reactions of hydrocarbons have been made, ranging from one-(or multi-)dimensional single particle models [50,68] to (semi-)detailed (multi-step) kinetic modelling [69,70], lumped kinetic models [70–72], simulation of turbulent reactive flows based on the eddy dissipation concept (EDC) [73,74] and studies of isolated reaction mechanisms (e.g., those of alkenes and alkanes) [75]. Even though oxygenated species formed from biomass decomposition may differ from fossil fuel-based hydrocarbons, the same relevant reactions can and will be considered in the following [76].

The oxidation mechanisms for hydrocarbons and n-alkanes involve complex chain radical processes with multiple reactions, intermediate radicals, and molecular species. Governing reactions are different classes of primary propagation reactions, including isomerization and β-decomposition of alkyl radicals, O_2 and H abstraction, O_2 addition, yielding peroxy radicals ($ROO^{\bullet}$, e.g., hydroperoxy $HO_2^{\bullet}$), and many more [77].

Considering, for instance, the oxidation of C_1 hydrocarbons in a simplified oxidation system, methane is attacked by $H^{\bullet}$, $O^{\bullet\bullet}$, and $^{\bullet}OH$ radicals, resulting in $^{\bullet}CH_3$ radicals. The $^{\bullet}CH_3$ partly recombines, yielding C_2H_6, C_2H_5, and C_2H_4 that again will be attacked by the respective radicals. Likewise, $^{\bullet}CH_3$ reacts with oxygen atoms to formaldehyde (CH_2O) and formaldehyde radicals ($^{\bullet}CHO$) by $H^{\bullet}$ abstraction. The latter can decompose to form CO, simultaneously forming $HO_2^{\bullet}$ or H_2, depending on the reaction partner (i.e., O_2 or $H^{\bullet}$) [75]. For higher hydrocarbons, the amount of possible formation, consumption, and recombination reactions increase enormously, still neglecting influencing parameters such as temperature, pressure, and system composition.

In the gas-phase, CO, whether as a primary product from hydrocarbon oxidation, fuel decomposition, or partial char oxidation, is further oxidized. This reaction is relatively slow compared to the preceding reactions [19,75,78]. Direct oxidation of CO (equation (13)), sometimes also referred to as “dry oxidation” as opposed to “wet oxidation” for the absence of hydrogen-containing compounds [79,80], is often considered a simplified global reaction for combustion modeling. However, although this reaction is possible, it will not be considered further in detail here; this reaction is substantially slower than reactions involving radicals [81], has a high activation energy, and is usually performed as a heterogenous reaction with metal catalysts [21–24,82].

$$2CO + O_2 \rightleftharpoons 2CO_2 \tag{13}$$

The actual prevailing reaction of CO oxidation in combustion systems (i.e., systems with H_2 and H_2O concentrations larger than 1 % [75]) follows the radical reaction pathways in the presence of a $^{\bullet}OH$ radical according to equation (14) [75,80,83].

$$CO + {}^{\bullet}OH \rightleftharpoons CO_2 + H^{\bullet} \tag{14}$$

Thus, to understand the mechanisms of hydrocarbon combustion as well as wet CO oxidation in detail, H_2–O_2 reaction submodel systems have to be considered, producing the radicals involved in the respective oxidation reactions. For radical reactions, once initiation reactions have occurred, chain branching, propagation reactions providing the radical pools, and termination reactions will take place. A summary of relevant reactions in H_2–O_2 and H_2–O_2–CO reaction systems is given by equation (15) - (21) [80,84–89]. In H_2–O_2 reaction systems, potential initiation reactions encompass the creation of alkyl radicals, unimolecular bond breaking resulting in the formation of two radicals [71], or the dissociation of hydrogen as illustrated in equation (15), where “M" denotes an unspecified third body component or collision partner, playing a role in supplying the necessary energy to stabilize the reactant combination. Usually, this reaction takes place at very high temperatures (>1700 °C). Still, since main reactions are based on chain propagation reactions, only a few initial radicals are required, making this not a rate-determining step [86]. Another initiation step is shown in equation (16) and usually occurs in higher-pressure systems under the formation of the stable hydroperoxy radical ($HO_2^{\bullet}$) [80,90].

$$H_2 + M \rightleftharpoons 2H^{\bullet} + M \tag{15}$$

$$H_2 + O_2 \rightleftharpoons HO_2^{\bullet} + H^{\bullet} \tag{16}$$

As for H_2–O_2 chain reactions, reaction (17) is most important – the reaction is strongly endothermic (thus slower at low temperatures), leading to further chain branching reactions forming $H^{\bullet}$, $O^{\bullet\bullet}$ (oxygen biradical), and $^{\bullet}OH$ radicals. Equations (17) and (18) are chain branching steps; two radicals are formed while only one is consumed. Chain termination steps can be due to wall collision [80,90] or the recombination of two radicals.

$$O_2 + H^{\bullet} \rightleftharpoons {}^{\bullet}OH + O^{\bullet\bullet} \tag{17}$$

$$H_2 + O^{\bullet\bullet} \rightleftharpoons {}^{\bullet}OH + H^{\bullet} \tag{18}$$

$$H_2 + {}^{\bullet}OH \rightleftharpoons H_2O + H^{\bullet} \tag{19}$$

$$H_2O + O^{\bullet\bullet} \rightleftharpoons 2\,{}^{\bullet}OH \tag{20}$$

$$H_2O + H^{\bullet} \rightleftharpoons {}^{\bullet}O\,H + H_2 \tag{21}$$

$$H^{\bullet} + O_2 + M \rightleftharpoons HO_2^{\bullet} + M \tag{22}$$

For the oxidation of CO, the concentration of hydroxyl radicals is essential, and reaction (14) prevails, as stated above. The radical reactions described by equation (23) - (26) are more or less significant alternative oxidation routes depending on the conditions within the combustion chamber. Reaction (26) for instance, may dominate in low-temperature regimes [77].

$$CO + O^{\bullet\bullet} \rightleftharpoons CO_2 \tag{23}$$

$$CO + O^{\bullet\bullet} + M \rightleftharpoons CO_2 + M \tag{24}$$

$$CO + O_2 \rightleftharpoons CO_2 + O^{\bullet\bullet} \tag{25}$$

$$CO + HO_2^{\bullet} \rightleftharpoons CO_2 + {}^{\bullet}O\,H \tag{26}$$

3. Parameters and compounds influencing CO emissions

After outlining the different mechanisms behind CO release during the complete thermo-chemical conversion of solid biofuels, the influential factors governing final CO concentrations in the gas-phase/flue gas of combustion processes will be depicted in the following chapters. In addition to fuel properties such as chemical composition, water content, and particle size [14,27,91], factors like combustion unit design and systems parameters, air-fuel ratio λ, temperature level, turbulence/mixing of the gas phase, residence time within the reaction zone [14–18], gas-phase composition and presence and concentrations of water/water vapor, CO_2, C_nH_m, $C_xH_yO_z$, and inorganic compounds significantly impact the concentration of the released CO and the final concentration of CO in the flue gas [11,58,92–94]. This is mainly due to two reasons.

- Chemical reaction mechanisms may be enhanced or inhibited depending on the concurring reactions and concentrations of participating elements.
- The occurrence of changes in equilibrium compositions might cause shifts in the balances of specific reactions.

However, reaching equilibrium is often unattainable due to (very) short residence times within combustion systems. Generally, Le Chatelier's principle can help predict some equilibrium systems' responses to external change, e.g., pressure, temperature, or concentration.

3.1. Influence of ambient conditions

Pressure. For domestic solid fuel appliance tests, specific draught requirements must be met according to DIN EN 16510-1 [95]. A minimum draught pressure of 12 Pa must be maintained during the nominal heat output test, while to meet the safety requirements, the natural draft pressure should not drop below 3 Pa during the entire test duration. Under actual conditions, 12 Pa is sometimes undershot but often exceeded [96–100]. A defined and controlled draught is usually realized in modern small and large-scale combustion units (e.g., forced or induced with ventilators and fans, as well as chimney draught regulators); (very) small-scale combustion units that operate without access to electricity, work with natural draught [15]. Depending on the furnace and the distribution of the combustion air within the combustion chamber, the draught conditions might strongly influence the efficiency and CO emissions [96,97,99]. The volume flow of the flue gas and the air supply changes depending on draught conditions, potentially resulting in:

- increased CO emissions in case of cooling effects from high excess air, lowering the temperature level (see next section) and influencing homogenous gas phase reactions, or
- reduced CO emissions for accelerated pyrolysis, gasification, and oxidation with higher oxygen supply.

Pressure variations within the combustion chamber of systems using solid biofuels can arise from factors such as pressure drop within the fuel bed due to pressure drops from dense fuel beds to the gas-phase, which might lead to the channeling of gases around the side walls, resulting in hot spots and higher emissions [91] and variables like particle size [27].

Temperature. Temperature influences all phases of thermo-chemical conversion realized during the full combustion (i.e., heating-up, pyrolytic decomposition, gasification, and oxidation; see chapter 2). Adiabatic combustion temperatures (i.e., temperatures a fuel theoretically reaches in case of complete combustion without heat loss) are lowered by increasing fuel moisture and ash content [101].

- For drying during the heating-up phase, sufficient temperature levels must be exhibited for water evaporation.
- In the phase of pyrolytic decomposition, elevated temperatures lead to greater yields of non-condensable gases, while lower temperatures result in higher quantities of char, tar, and other condensable products [102,103].
- Heterogenous reactions taking place during the gasification phase also respond to temperature variations; notably for endothermic char steam reforming (4) and the Boudouard reaction (3), CO and H_2, and CO, respectively, are favored as the temperature rises (and pressure decreases) [104].
- Secondary homogenous gas-phase reactions (phase oxidation) transforming and oxidizing long-chained hydrocarbons (i.e., tars) to CO and H_2 are most pronounced in higher temperature ranges [19].

Chen et al. [58] conducted a reactive force fields (ReaxFF) model simulation of the combustion process of solid biofuels under various conditions, including different temperatures, oxidative levels, and humidity. They observed that CO_2 production is favored at lower temperatures, while CO production is facilitated at higher temperatures. This also aligns with the behavior from char gasification (see chapter 2), where lower temperatures promote the release of CO_2 from char gasification, while higher temperatures shift concentrations towards CO [58,59,61].

The oxidation of CO to CO_2 necessitates elevated temperature levels [15,80]. In contrast, high temperatures, although independent from pressure, shift reactions such as the exothermic water-gas-shift reaction (27) towards CO and H_2O [104].

$$CO + H_2O \leftrightharpoons CO_2 + H_2 \tag{27}$$

3.2. Influence of gas phase composition

Oxygen (O_2). In thermo-chemical conversion systems, the minimal oxygen demand determines the amount of oxygen/air necessary for complete oxidation (i.e., to H_2O and CO_2). The air-fuel ratio λ expresses the mass ratio of actual and minimal air demand in such a system and needs to be > 1 for sufficient oxygen availability; for overoxidized systems, the energy losses and temperature drops due to the heating of excessive gas must be accounted for [80].

Su et al. [49] investigated the emission behavior of CO and CO_2 of milled pine wood in thermogravimetric analysis (TGA) experiments. The temperature was set from ambient temperatures to 800 °C, and the atmosphere (mixture of argon and oxygen) shows oxygen concentrations of 0 %, 5 %, 10 %, 15 %, and 21 %. Regarding the evolution of CO and CO_2 from the pyrolytic decomposition and gasification of solid biofuels, cumulative emissions of both CO and CO_2 increase with an increasing oxygen content within the ambient atmosphere. However, the behavior of the CO to CO_2 ratio differs depending on the oxygen concentration: the highest ratio of CO/CO_2 is reached without oxygen (i.e., O_2 concentration of 0 %, where the oxygen comes only from the solid biofuel) and reaches a minimum at 10 % O_2 [49]. This phenomenon can be attributed to the low oxygen concentration, not effectively reaching the particle surface due to volatile efflux and the boundary layer (chapter 2). As a result, oxygen remains in the gas-phase and reacts with the released decomposition (and gasification) products, enhancing the oxidation of CO and C_nH_m, leading to higher amounts of CO_2. For higher concentrations (i.e., oxygen concentrations of 15 % and 20 % [49]), more O_2 molecules overcome the boundary layer, leading to increased reactions with the remaining solid coke/char as well as exothermic reactions with the solid char/coke, eventually promoting endothermic reactions resulting in proportionally more CO (Le Chatelier's principle).

For homogenous gas-phase reactions, Chanpirak et al. [105] also showed inhibited CO oxidation for 5 % compared to 0.75 % O_2 in a system consisting only of CO–O_2–H_2O as reactants. They explained this with reaction (22) being the rate-limiting step for these O_2 levels, competing with the chain branching reaction (17) and the formation of $HO_2^\bullet$ as a relatively unreactive radical compared to $^\bullet OH$ from reaction (22). Chen et al. [58] observed in reactive force fields (ReaxFF) model simulations that higher concentrations of O_2 (fuel-lean conditions) led to increased lignocellulosic biomass decomposition. In comparison, fuel-rich conditions resulted in higher concentrations of H_2 and CO. Additionally, more CO formation occurred under a mixed H_2O/O_2 atmosphere [58].

Moisture (H_2O). Adiabatic combustion temperatures might be lowered due to the moisture content of the fuel, as the energy required for evaporation must be considered. Higher moisture content evidently results in a higher moisture evaporation rate and lower devolatilization rate, which is strongly dependent on the temperature: higher moisture in fuels leads to a higher heat demand for evaporation, leaving less heat for the devolatilization within the fuel and eventually to a reduced devolatilization rate leading to an overall decreased burning efficiency and higher CO emissions [14]. Char gasification, on the contrary, may be intensified for higher moisture contents, since O_2 consumption is lower due to the reduced devolatilization rate. Very low moisture contents in fuels (i.e., <3.3 wt.-%) have been reported to cause higher CO and TPM emissions in pellet stoves [27,92]. This can be explained by the necessary radical pool in section 2.3: the radicals $^\bullet OH$, $H^\bullet$, and $O^{\bullet\bullet}$ are vital for homogenous gas-phase oxidation reactions. High levels of H_2O vapor have been reported to promote the oxidation of CO due to the formation of $^{\bullet}$OH radicals [92]. On the other hand, extremely dry fuel conditions and a low hydrogen content within the fuel may result in a low O/H radical pool, leading to insufficient combustion and CO oxidation [15].

CO_2 and (Oxygenated) Hydrocarbons (C_nH_m and $C_xH_yO_z$). The reactive force fields (ReaxFF) study [58] also reported more H_2O and fewer H_2 molecules being generated from biomass decomposition and gasification with increasing CO_2 concentrations. All findings are attributable to the equilibrium concentrations of reaction (14), as well as the concurrent radical formation reaction (17), where $H^{\bullet}$ radicals compete with the reverse reaction (14). Reaction (22) also becomes more prominent in fuel-lean conditions [92].

In combustion processes, particularly in homogenous gas-phase reactions for hydrocarbon oxidation, CO is the principal primary product. The gas-phase oxidation of CO to CO_2 occurs later, often not until the complete consumption/conversion of the initial fuel and intermediate hydrocarbon fragments, since the latter is faster than the CO oxidation and also competes for $^{\bullet}$OH radicals [80]. Consequently, the presence of partially or incompletely oxidized compounds like C_nH_m and $C_xH_yO_z$ result in elevated CO concentrations.

Studies have also investigated the impact of CO_2 on the gas-phase oxidation behavior of CO to CO_2. High CO_2 concentrations have been reported to inhibit CO oxidation, more prominent in the presence of higher H_2O concentrations in the gas-phase [92].

3.3. *Influence of inorganic components*

As lignocellulosic biomass degrades and undergoes volatilization, it releases not only organic elements but also alkali, alkaline earth metals, and compounds containing these metals into the surrounding gas phase. This results in the emission of inorganic particulates influencing the thermo-chemical conversion properties, the conversion efficiency, the slagging and fouling behavior, as well as the corrosion activities [106–109]. The impact of these effects is closely linked to the concentrations of these elements, which, in turn, vary depending on the type of solid biomass being used. For instance, herbaceous biomass generally exhibits higher levels of inorganic compounds than wood. Especially inorganic elements (i.e., d-block elements as well as alkali and alkaline earth metals) have catalytic effects on the decomposition and gasification of lignocellulosic biomass as well as on gas-phase reactions [59, 105].

3.3.1. *Elemental associations and release of inorganic components*

Although only the overall elemental content is often considered, the chemical form and association of these elements within the solid biofuel or plant tissues are essential for the underlying phenomena and challenges they provoke. Types of association of these elements can be in the form of dissolved salts, organically bound species, included/incorporated mineral matter, and excluded/unincorporated mineral matter [110]. The firsts are found as ions (e.g., K^+, Na^+, Ca^{2+}, Cl^-, SO_4^{2-}) in the fluid matter inside the plants, accumulating as precipitated salts. Organically bound species (i.e., K^+, Na^+, Ca^{2+}, Mg^{2+}, Fe^{3+}, Al^{3+} as well as covalently bound S, P, and Cl) are mostly oxalates undergoing intricate conversions leading to inorganic residues after combustion. Incorporated mineral matter consists of distinct inorganic particles containing Ca, Mg, and Si. At the same time, unincorporated materials include aluminosilicates (abundant in K, Na, Ca, and Fe), feldspars, and quartz originating from soil contamination [110]. In lignocellulosic biomass, more than 90 % of alkali metals are present in the form of water-soluble and ion-exchangeable forms, making them readily available for release during thermo-chemical conversion [111]. Especially K and Na mainly occur in the form of salts (e.g., chlorides, acetates, sulfates, and others).

The decomposition of alkali metals in solid biomass varies based on their presence within organic or inorganic components [112], and transformation occurs during the devolatilization and char conversion phases. In lower temperature ranges, alkali metals associated with the organic phase (e.g., alkaline carboxylates or phenol-associated alkali metals [113]) are released as devolatilization occurs, whereas for temperatures above 500 °C inorganic metals (e.g., KCl for K) evaporate [114]. At higher temperatures, reactions with K-silicates or aluminosilicates occur and are dominant during devolatilization and char burnout, though dependent on Si, Cl, and divalent cations (i.e., Ca^{2+} and Mg^{2+}) [113]. For fuels that contain high levels of Cl, like straw, alkali metals tend to be released as alkali chloride (e.g., KCl). In contrast, in fuels with low chlorine (and low alkali) content, such as wood, alkali metals are released through vaporization as alkali sulfates (e.g., K_2SO_4), and alkali hydroxides (e.g., KOH) [115]. Inorganic compounds in the char can also contribute to the formation of carbonates (e.g., K_2CO_3 in the presence of CO_2 [112]), hydroxides (e.g., KOH in the presence of water vapor), sulfates, and silicates.

3.3.2. *Influence on thermo-chemical conversion*

The following section will outline the influences of the primary inorganic elements and metals during the thermo-chemical conversion of solid biofuels.

3.3.2.1. *Pyrolytic decomposition.* Metals are known to act as catalysts and exhibit catalytic properties in lignocellulosic biomass decomposition. Although research has focused on investigating the effects of metals on cellulose, hemicellulose, and lignin [110] rather than biomass as a whole, effects related to these metals have been evaluated. The experiments are usually conducted on raw samples versus those treated with HCl and H_2O to reduce alkali metal content (e.g., Refs. [113,116,117]). Notably, these evaluations reveal that the presence of alkali and alkaline earth metals during the pyrolytic decomposition phase results in gas compositions featuring lower CO concentrations and elevated CO_2 contents [118,119]. Alkali and alkaline earth metals have proven to accelerate the onset of decomposition reactions and the maximum temperature of the degassing rate, promoting decomposition pathways leading to higher yields of low molecular weight condensable compounds and permanent gases (e.g., CO and CO_2) and positively affecting char reactivity [110].

K, in particular, is often referred to as the most relevant species for catalytic reactions in lignocellulosic matter. This is not only because of the overall amount present typically in biomass but also due to its high catalytic activity during thermo-chemical conversion. The impact of K in heterogeneous catalysis primarily involves the creation of oxygen-containing functional groups and the conversion of small ring molecules into more complex ring systems [93]. K has also been noted to promote the breakdown of cellulose chains during the pyrolytic decomposition of wood [120]. There is no consensus in the literature about the active intermediate functioning as catalysts, but the proposed species for K include K_xO_y, K_2O, K–O–C, K–C, and C_nK (see Refs. [93, 121]).

3.3.2.2. *Heterogenous solid-gas reactions.* In biomass gasification with CO_2 and H_2O as oxidizing agents, heterogenous catalytic controlled reactions involve oxygen transfer, active site mechanisms, and desorption mechanisms. Alkali and alkaline earth metals, mostly solid alkali metals in the char [122], catalyze the (steam) gasification reactions (2) and (3) by CO_2 and H_2O, respectively, most likely by the creation of active sites and by catalyzing the subsequent desorption of CO [93]. Parts of alkali metals are released into the gas-phase as volatiles, while the solid-phase alkali metals remain within the char. At the same time, the char is surrounded by volatile substances, including volatile alkali metals. The vaporized alkali metals may simultaneously adsorb and migrate to the char's surface, partly diffusing through the internal pores. With oxygen, they create stable oxygen-containing structures, which exhibit superior catalytic activity compared to the alkali metal residues remaining in the char [114,123].

3.3.2.3. Homogenous gas-phase reactions. In homogenous gas-phase reactions, alkali and alkaline earth metals, especially the alkali metal and more specifically K, as well as other elements (e.g., sulfur oxides, nitrogen oxides, chlorine species), affect reaction pathways, product formation, equilibrium, and combustion efficiency. This is true even if they are only present as trace species [94]. This may arise from either direct chemical reactions of these elements or interactions with the radical pool.

These interactions can result in a range of different effects on CO oxidation, where some reactions may enhance the process while others might inhibit it. The outcome depends on which overall reaction pathway dominates under the actual given specific conditions (e.g. Refs. [94,105,113,124–129]).

Catalytically enhancing reactions of trace species (T) in the gas-phase can occur due to the radical branching reactions (28) and (29). X and Y represent $H^{\bullet}$, $^{\bullet}OH$, $O^{\bullet\bullet}$ or alkyl radicals. The reverse reactions terminate radical chain reactions [94].

$$T + XY \leftrightharpoons TX + Y \tag{28}$$

$$TX\ (+M) \leftrightharpoons T + X\ (+M) \tag{29}$$

Potassium (K). Alkali metals play a significant role in gaseous combustion and can act in two ways: as promoters or inhibitors. Their inhibitory effect is related to flame propagation inhibition and the catalytic removal of radicals, while the promotion effects arise from the reverse (inhibition) reaction sequences, thus promoting radical formation [94].

K from solid biomass combustion may be released as KCl, KOH, and K_2SO_4. Gaseous KCl and KOH react mainly with $H^{\bullet}$ to form atomic K and HCl/H_2O (reactions (30) and (31)). Atomic K reacts with $^{\bullet}OH$ radicals and O_2, forming KOH and $KO_2^{\bullet}$, from which the latter may also react with $^{\bullet}OH$ radicals to form KOH. K_2SO_4 may follow nucleation to form aerosols like KCl, leading to PM emissions [108]. However, unlike KOH and KCl, no interactions with radicals have been reported for K_2SO_4 [105]. This is why the presence of sulfur may reduce the inhibition of CO oxidation: sulfur reduces the formation of K atoms by sulfating KCl/KOH to K_2SO_4 [124]. For KOH and KCl, the radical removal follows the reactions (30) - (34), where (30) and (32) correspond to the reverse reactions of equations (28) and (29) [129].

$$KOH + H^{\bullet} \leftrightharpoons K^{\bullet} + H_2O \tag{30}$$

$$KCl + H^{\bullet} \leftrightharpoons K^{\bullet} + HCl \tag{31}$$

$$K^{\bullet} + {}^{\bullet}O\ H + M \leftrightharpoons KOH + M \tag{32}$$

$$K^{\bullet} + O_2 + M \leftrightharpoons KO_2^{\bullet} + M \tag{33}$$

$$KO_2^{\bullet} + {}^{\bullet}O\ H \leftrightharpoons KOH + O_2 \tag{34}$$

Other homogenous catalytic mechanisms involve mostly gaseous alkali metals. Steam tends to react more with thermally stable macromolecular compounds within the volatiles, resulting in an increased gas yield. Moreover, KCl is reported to activate and facilitate the water-gas shift reaction [93].

Nitrogen (N). Even in small amounts, NO substantially influences the oxidation of H_2, C_nH_m, $C_xH_yO_z$, and notably CO. Nitrogen oxides in combustion can result either from thermal formation pathways (thermal NO_x, generated at high temperatures through the reaction of molecular nitrogen and oxygen from the combustion air), in the presence of hydrocarbon radicals (prompt NO_x), via N_2O intermediates or from chemically bound N of the biofuel (e.g., from amines), often involving $H^{\bullet}$, $^{\bullet}OH$, and $O^{\bullet\bullet}$ radicals. Typically, high oxygen levels and high temperatures promote fuel burnout but contribute to increased NO_x emissions [19].

Small NO concentrations in the gas-phase (i.e., 50 to 1000 ppm) may promote the oxidation of CO by enhancing the conversion of $HO_2^{\bullet}$ into more reactive $^{\bullet}OH$ radicals through reaction (35). At elevated NO concentrations or under reducing conditions, NO can hinder the oxidation process by causing $H^{\bullet}$ recombination, leading to a delay in CO oxidation (reactions (36) and (37)) [94,128].

$$NO + HO_2^{\bullet} \leftrightharpoons NO_2 + {}^{\bullet}OH \tag{35}$$

$$X + NO + M \leftrightharpoons XNO + M \tag{36}$$

$$Y + XNO \leftrightharpoons XY + NO \tag{37}$$

Sulfur (S). S usually has a subordinate significance in solid biofuel combustion due to a mostly low content within lignocellulosic material. S from biomass can be bound within the ash as mostly sulfates or released as gaseous components (e.g., H_2S). The oxidation of H_2S leads to SO_x composed mainly of SO_2 and, in small amounts, SO_3. SO_x is formed via complex radical reaction routes involving $H^{\bullet}$, $^{\bullet}OH$, $O^{\bullet\bullet}$ and intermediate species such as, e.g., $^{\bullet}SH$, SO, and $HSO^{\bullet}$ [19].

The introduction of SO_2 leads to a minor inhibition of CO oxidation [105], showing that SO_2 also acts as a radical sink, primarily due to reactions with $O^{\bullet\bullet}$. Radical reactions with $^{\bullet}OH$ play a small role due to the instability of the intermediate product $HOSO_2^{\bullet}$, dissociating back to $^{\bullet}OH$ and SO_2 [127]. In systems where K is present, small amounts of SO_2 can drastically decrease the CO emissions by indirectly interacting with the radical pool and binding compounds concurring with radicals for oxidation, e.g., by binding KCl and KOH to K_2SO_4, which, contrary to KCl and KOH, does not promote radical recombination according to the reactions (30) - (34) [105]. The overall reactions of K_2SO_4 from KCl and KOH involving SO_2 and SO_3, the latter formed by oxidation of SO_2, are shown in reactions (38) and (39), respectively [105,124,129]. The sulfation of KOH occurs more easily than the sulfation of KCl [105].

$$2KCl + SO_2 + \tfrac{1}{2}O_2 + H_2O \leftrightharpoons K_2SO_4 + 2HCl \tag{38}$$

$$2KOH + SO_3 + M \leftrightharpoons K_2SO_4 + H_2O + M \tag{39}$$

Chlorine (Cl). Cl is particularly relevant for herbaceous biomass and is present primarily in the form of alkali salts (e.g., KCl, NaCl) [19]. During combustion, Cl undergoes an almost complete transition to the vapor phase as alkali chloride or hydrogen chloride (HCl) [16]. Cl inhibits ignition and flame speed while promoting flame quenching in gas-phase combustion.

Compounds like HCl and chlorinated hydrocarbons have been found to hinder the oxidation of CO. The interaction of chlorine with the radical pool is intricate, and its overall impact is determined by the interplay between competing chain termination and chain propagating steps [94]. In regards to the interaction with K and its inhibitory effects, higher concentrations of Cl lead to the conversion of K to KCl, resulting in lower amounts of K atoms in hot gas and lower CO and H_2 concentrations, eliminating the inhibition effects of K on CO and H_2 oxidation [124]. At the same time, inhibitory effects of KOH and KCl on moist CO oxidation have been reported.

4. Fuel-related measures for CO emission reduction

Different measures are possible for the reduction of CO release. The following outlines primary measures (on the fuel side) for gaseous emission reduction.

4.1. Biofuel properties

The physical-mechanical properties of solid biofuels have a significant impact on the emissions generated during combustion. This influence depends e.g., on the form of the fuel (e.g., wood logs, pellets, briquettes). Another critical characteristic affecting emissions from biofuel combustion is the water content of the fuel. High fuel moisture leads to lower temperatures in the combustion chamber and lower efficiency. In parallel, water can act as a catalyst in hydrocarbon and volatile oxidation within the gas phase [80], providing radicals for fuel oxidation. Therefore, very dry fuel may again lead to a decrease in conversion efficiency [11]. Another adjustable influenceable property of biofuels is the particle size of the fuel; larger particles show thermal insulation properties and therefore a lower devolatilization rate compared to smaller particles [91].

The chemical composition of the fuel is also crucial. To change the overall composition, a co-combustion with less “critical” fuels can be carried out (i.e., fuels with lower inorganics such as alkali and alkaline earth metals, Cl, S, and N). Additionally, a pre-treatment such as acid and/or water leaching/washing is possible. These approaches can help mitigate deposition and corrosion issues during combustion by modifying the ash behavior, retaining inorganic volatiles within the ash, and by adjusting the different ratios of elemental compositions [12].

Fuel indices have been developed, considering the physical behavior, the chemical reaction pathways, and the interactions between elements. These indices provide information on the extent of gaseous pollutant emissions (e.g., the N content for NO_x or the molar $(K + Na)/(2S + Cl)$ ratio for HCl and SO_x emission potential) and also address ash issues, including inorganic particle emissions [130]. For the latter, the sum of K, Na, Zn, and Pb indicates the aerosol emissions; during combustion, these semi-volatile and volatile ash-forming elements are released into the gas phase, where they nucleate (homogenously and heterogeneously) and condensate heterogeneously, forming aerosols and PM emissions [131]. Since K usually reveals the highest concentrations of the elements mentioned above, the molar Si/K and Cl/Si ratios additionally indicate K release. High Si/K ratios suggest a reduced release of K due to the formation of K silicates [130]. At temperatures above 500 °C, Cl has been reported to enhance alkali metal release from solid biomass [111]. Thus, increasing Cl/Si ratios in combustion processes might imply a higher release of K. The S/Cl ratio is an indicator of high corrosion risk; high ratios (i.e., $S/Cl > 4$) point to the formation of protective sulfate layers on the inner surfaces of the combustion unit [130,132]. These indices can also help estimate the CO emissions in biomass combustion systems by estimating the evolution, formation, and retention within the ash of influencing compounds and elements.

4.2. Fuel pre-treatment

One approach to improving the combustion properties of lignocellulosic biomass is washing or leaching it with water or (diluted) acids. In biomass leaching, the aim is to extract water-soluble elements from the biomass, thus reducing corrosion and slagging properties during combustion, increasing ash melting temperatures, and reducing TPM-forming elements. Components of ash-forming substances and salts K, Na, Ca, Mg, Cl, S, P, and N, present in the form of ions (e.g., K^+, Na^+, Ca^{2+}, Mg^{2+}, NH_4^+ and Cl^-, SO_4^{2-}, PO_4^{3-}, HPO_4^{2-}) and partly Si, Ti and Al are thus discharged from the biomass by washing [12,133,134].

In literature, the effects on the combustion behavior of pre-treated lignocellulosic biomass are primarily reported regarding ash (melting) behavior, slagging, and agglomeration [135,136]. Regarding gaseous emission reduction, only within a limited number of studies airborne emissions of treated and untreated material are compared. Dayton et al. [137] measured the release of inorganic constituents as well as CO, CO_2, and NO from leached straw samples during combustion and reported a lack of HCl and alkali metal vapors and a similar amount of released CO_2 and NO for leached straw compared to untreated straw. On the contrary, CO was released about 12 times less during combustion, and the char combustion phase was four times shorter for untreated straw. In a study by Rachivhandran et al. [138], CO reduction of 50 % for leached agricultural biomass briquettes as opposed to unleached briquettes was observed in domestic wood stoves. Schmidt et al. [29] reported a decrease in CO emissions between 32 % and 48 % for washed fir, beech, and oak pellets in a 6.3 kW pellet stove. They attributed this to the reduction of K, favoring the gasification of cellulose when present [139].

4.3. Fuel additivation

The addition of catalysts in solid fuel combustion aims to enhance burnout and reaction kinetics while adding additives to the solid biomass might target several mitigation issues (e.g., total particulate matter (TPM) emissions, corrosion, slagging, fouling). In the following, both possibilities are outlined.

4.3.1. Catalytic combustion

Catalysts can be either used as secondary measures for downstream flue gas treatment or, though less frequently applied, by the addition of catalysts to the fuel. Catalytic combustion, referring to the latter, may enhance combustion performance and efficiency, reduce emissions from incomplete combustion, decrease ignition temperature, and increase combustion rates [140]. Alkali, alkaline earth metals and transition metals have been used for this [25,140–146]; however, due to the high costs of the latter, their wider use is highly unlikely.

The catalytic effects result from the oxygen storage and redox properties of metal oxides and, in the case of salts, from the first ionization energy, leading to improved oxygen transfer behavior [140,143]. The results from Wang et al. [141] and Vamvuka et al. [140] show that ignition and combustion temperatures (i.e., peak and burnout temperatures in the TGA) were lowered with TiO, CuO, and MnO during wheat straw combustion [141] and LiCl, NaCl, MgO, CaO, TiO_2, V_2O_5, Fe_2O_3, and CuO during lignite and residual biomass (i.e., olive tree pruning, cardoon, and sewage sludge [140]) combustion. Biomass has more volatiles compared to coal [143]; thus, the positive effect on the burnout quality, as reported for coal, might be compensated by the inhibitory effects of alkali metals in the gas phase burnout for biomass. Nonetheless, catalytic combustion kinetics of alkali metal treated biomass (e.g., rice hull and bamboo [143]) have been investigated, reporting reduced devolatilization temperatures, increased combustibility index, and increased differential thermal peak area (DTG Analysis). Gaseous emissions from alkali metal-treated biomass combustion have not been reported so far.

4.3.2. Solid mineral additivation

Solid additives interact and react with components present in the biomass, inducing alterations in the chemical composition of the resulting ash. This leads to changes in the ash melting temperature and binds alkali metals from volatile components (e.g., alkali chlorides and alkali sulfates) within the ash, reducing alkali- (and silicate melt-) induced slagging and agglomeration [147]. Regarding TPM and, more particularly, PM, which primarily originate from K and, to a lesser extent, from Na, for complete combustion, high mitigation potentials have been demonstrated [148]. Typical solid additives include those based on Al, Ca, P, and S, while less common options are Mg-, Zn-, and Fe-based [12] and work by various mechanisms of action, often in synergy. The following main effects can be distinguished.

- Chemical effects. Through (irreversible) chemical reactions with the additives, low-temperature melting, highly volatile, ash- and PM-forming elements from the biomass can be converted into high-temperature stable compounds, remaining in the solid combustion residue or ash.
- Physical effects. Volatile, condensable and/or molten or liquid elements or compounds of the biomass can be adsorbed by suitable porous additives with large specific surface area. In addition, the ash melting temperature of solid biofuels can be increased by the addition of inert, high-temperature stable additives.

The effect and efficiency of the respective additives depend on the chemical composition of biomass and additive, as well as the additive concentration, leading to different mass and molar ratios in the biomass combustion system. The Al–Si-based mineral Kaolinite ($Al_2Si_2O_5(OH)_4$) is often considered an effective additive (e.g., Refs. [148–153]), primarily functioning through chemical adsorption and reaction mechanisms. It reduces the release of K by binding KCl, K_2SO_4, and KOH into stable K–Al–Si compounds, notably leucite ($KAlSi_2O_6$, with a melting temperature of $T_m > 1500$ °C) and kalsilite ($KAlSiO_4$, $T_m > 1600$ °C) [154]. The reaction equations are depicted in equation (40) - (43).

$$Al_2Si_2O_5(OH)_4 + 2KCl \rightarrow 2KAlSiO_4 + 2HCl + H_2O \tag{40}$$

$$Al_2Si_2O_5(OH)_4 + K_2SO_4 \rightarrow 2KAlSiO_4 + SO_3 + 2H_2O \tag{41}$$

$$Al_2Si_2O_5(OH)_4 + 2KCl + 2SiO_2 \rightarrow 2KAlSi_2O_6 + 2HCl + H_2O \tag{42}$$

$$Al_2Si_2O_5(OH)_4 + K_2SO_4 + 2SiO_2 \rightarrow 2KAlSi_2O_6 + SO_3 + 2H_2O \tag{43}$$

Ca-based additives (e.g., CaO, $CaCO_3$, $Ca(OH)_2$) primarily operate through chemical adsorption and reaction mechanisms, as well as the increase of melting points and dilution effects. They capture predominantly Cl and S. When used in suitable quantities, they may retain K as Ca–K compounds. However, excessively high concentrations of calcium-based additives might inadvertently enhance K release [155]. (Solid) additives with S-containing compounds sulfate alkali chlorides and hydroxides (as discussed above for homogenous gas phase reactions) in order to reduce the risk of corrosion [148]. Although CO emission reductions were not a direct focus in the conducted studies for fuel additivation and therefore not always reported, published data show significant reductions of up to 90 %. Especially for the case of kaolin (mainly consisting of kaolinite) as an additive, high reduction potentials have been reported (e.g., Refs. [11,151,152,156]), some of which show a strong link between K removal from the flue gas [9,157]. The underlying mechanisms for this phenomenon have not been thoroughly investigated or understood, although some explanations in the case of kaolin attribute this to possible catalytic effects of kaolin, improved fire bed structure due to K-silicates embedded in the ash, preventing channeling and the formation of CO layers [11]. Another explanation is that the reduction of K release into the gas phase due to binding K into stable K–Al–Si-compounds in the ash mitigates the interference of K on CO and hydrocarbon oxidation [157]. Similar conclusions have been drawn from biomass gasifiers using olivine, where the decrease in CO emissions was linked to the incorporation of K into silicate structures, confirming the role of K as an inhibitor for CO oxidation in their study [158]. In other 12 MW_{th} experiments with Circulating Fluidized Bed (CFB) boiler using silica-sand and Linz-Donawitz (LD)-slag as bed materials, the authors attributed the rising CO emissions to the poor ash absorption capabilities of LD-slag, hindering alkali removal from the boiler [159, 160].

4.3.3. (Gaseous) sulfur additivation

While solid additivation prevents the release of K-containing compounds, the addition of gaseous components (e.g., SO_2) or solid precursor substances for gaseous components (e.g., elemental S and ammonium sulfate ($(NH_4)_2SO_4$) [159]) leads to an increased S/Cl ratio and reactions with K-compounds such as KOH and KCl. These compounds are sulfated into less corrosive K_2SO_4 (reactions (38) and (39)) [132] and also do not interfere with the radical pool, thus enhancing the CO oxidation rate [105]. However, SO_2 may lead to high-temperature corrosion of several metals and the increased need for flue gas cleaning [132]. Thus, the addition of S(-compounds) is not an established method and only a limited number of studies have been published on this subject. For example, in a 2 to 4 MW_{th} dual fluidized bed gasifier system, elemental S was introduced into the boiler fuel feed [161]. Part of the solid fuel is converted within this gasifier into a product gas, while the rest is combusted in a connected boiler to meet the heat demands of the allothermal gasifier (see Refs. [162,163]). Here, a decrease in tar content, increased H_2 and CO_2 yield of the system, as well as an increased H_2S yield were reported [161]. The latter is attributed to the sulfation of K to K_2SO_4 in the boiler, which then is transported to the gasifier and decomposed to H_2S and catalytically active KOH and K_2CO_3. Another approach involves the addition of ammonium sulfate ($(NH_4)_2SO_4$), which can be added to the afterburn chamber [164] or sprayed into the cyclone outlet [159] and has been reported to effectively reduce gaseous KCl and CO emissions, respectively. Elemental sulfur must be first oxidized to SO_2 and subsequently to SO_3 (equations (44) and (45)). This reaction is slow in temperature ranges below 900 °C [165]. In the case of $(NH_4)_2SO_4$, it is decomposed directly to SO_3 and NH_3 (equation (46)).

$$S + O_2 \rightarrow SO_2 \tag{44}$$

$$SO_2 + \tfrac{1}{2}O_2 \leftrightharpoons SO_3 \tag{45}$$

$$(NH_4)_2SO_4 \rightarrow 2NH_3 + SO_3 + H_2O \tag{46}$$

5. Conclusion

Minimizing CO emissions in combustion processes is desirable due to its toxicity and to improve combustion efficiency; additionally, CO emissions are in some countries legally limited. These CO emissions result from incomplete combustion and are formed during the thermo-chemical conversion phases “pyrolytic decomposition”, “gasification” of the residual carbon/coke, and/or during “oxidation” of the released volatiles and gases. The main steps for CO formation in biomass combustion and the influence of temperature, alkali (precisely K), and alkaline earth metals are summarized below.

- During pyrolytic decomposition, CO results mainly from cracking and reforming of ether bonds (C–O–C) and carbonyl groups carbonyl (-C═O) and from cleavage of carboxyl (-COOH) and formyl (-CHO) fragments and radicals. During combustion, CO mainly originates from cellulose and less from hemicellulose and lignin. Higher temperatures during the thermo-chemical conversion provide a greater yield of non-condensable gases (e.g., CO, CO_2, CH_4, H_2). Alkali and alkaline earth metals accelerate the pyrolytic decomposition reactions, leading to higher yields of condensable products with low molecular weight and permanent gases (e.g., CO and CO_2). The metals form intermediate groups, functioning as catalysts.
- Transport phenomena and ad- and desorption kinetics significantly influence heterogeneous solid-gas reactions (phase gasification). Lower temperatures favor the formation of CO_2, whereas higher temperatures promote CO formation; i.e., endothermic, heterogeneous reactions like steam reforming and the Boudouard reaction leading to CO are favored in higher temperature regimes. Alkali metals catalyze steam gasification reactions by catalyzing the desorption of CO.
- In homogenous gas phase reactions (phase oxidation), previously emitted hydrocarbons and other volatiles are rapidly oxidized, leading to CO as a primary product from hydrocarbon oxidation. CO oxidation in the gas phase occurs mainly with $^{\bullet}OH$ radicals; i.e., radical reaction pathways are essential. Gas phase reactions and CO oxidation are generally promoted at higher temperatures. Alkali metals (e.g., K in the form of KCl and KOH) inhibit CO oxidation by removing $^{\bullet}OH$ radicals from the radical pool, limiting available radicals for CO oxidation.

Numerous fuel-related measures for the mitigation of CO emissions, or rather the complete oxidation of those, are possible. This can be an alteration and modification of the fuel and its chemical composition, as well as the addition of supplementary compounds. Depending on the underlying mechanism of the respective measure, one way to minimize CO emissions is maintaining a high radical availability by reducing their interference with alkali compounds, i.e., mostly K, within the gas phase. This can be a result of either:

- The suppression of K-release into the gas phase. This can be realized by minimizing the respective content within the solid biofuel (e.g., through washing) or binding K in temperature-stable compounds within the ash (e.g., due to mineral additivation). Thus, inhibition of CO oxidation due to K interference with the radical pool is minimized.
- K release into the gas phase, but CO inhibition effects are diminished due to gas-phase reactions with K (e.g., due to the sulfation of K to K_2SO_4, which does not interfere with the radical pool).

Minimizing CO emissions by fuel-related measures can be achieved by reducing the interference of compounds with O/H radicals while maximizing the radical pool. This can be accomplished by several measures, ranging from fuel pre-treatment to the introduction of additives. In various practical installations, the utilization of solid additives has proven to be the most effective approach.

Declaration of competing interest

The authors declare that they have no known competing financial interests or personal relationships that could have appeared to influence the work reported in this paper.

References

[1] Umweltbundesamt: Erneuerbare Energien in Deutschland, Daten zur Entwicklung im Jahr 2022, 2023.
[2] Umweltbundesamt: Heizen mit Holz - Ein Ratgeber zum richtigen und emissionsarmen Heizen mit Holz.
[3] M. Banja, R. Sikkema, M. Jégard, V. Motola, J.-F. Dallemand, Biomass for energy in the EU – the support framework, Energy Pol. 131 (2019) 215–228, https://doi.org/10.1016/j.enpol.2019.04.038.
[4] BMWK Bundesministerium für Wirtschaft und Klimaschutz: Auf einen Blick: Die neue Förderung für den Heizungstausch - Unterstützung für die Wärmewende. https://www.energiewechsel.de/KAENEF/Redaktion/DE/Downloads/foerderung-heizungstausch-beg.pdf?__blob=publicationFile&v=23, 2024.
[5] IEA, International Energy Agency: Net Zero by 2050 - A Roadmap for the Global Energy Sector.
[6] L.S. Bäfver, M. Rönnbäck, B. Leckner, F. Claesson, C. Tullin, Particle emission from combustion of oat grain and its potential reduction by addition of limestone or kaolin, Fuel Process. Technol. 90 (2009) 353–359, https://doi.org/10.1016/j.fuproc.2008.10.006, 3, S.
[7] W. Cheng, Y. Zhu, J. Shao, W. Zhang, G. Wu, H. Jiang, J. Hu, Z. Huang, H. Yang, H. Chen, Mitigation of ultrafine particulate matter emission from agricultural biomass pellet combustion by the additive of phosphoric acid modified kaolin, Renew. Energy 172 (2021) 177–187, https://doi.org/10.1016/j.renene.2021.03.041. S.
[8] M. Gehrig, M. Wöhler, S. Pelz, J. Steinbrink, H. Thorwarth, Kaolin as additive in wood pellet combustion with several mixtures of spruce and short-rotation-coppice willow and its influence on emissions and ashes, Fuel 235 (2019) 610–616, https://doi.org/10.1016/j.fuel.2018.08.028. S.
[9] C. Gollmer, V. Weigel, M. Kaltschmitt, Emission mitigation by aluminum-silicate-based fuel additivation of wood chips with kaolin and kaolinite, Energies 16 (2023) 3095, https://doi.org/10.3390/en16073095, 7, S.
[10] I. Höfer, T. Huelsmann, M. Kaltschmitt, Influence of Ca- and Al-additives on the pollutant emissions from blends of wood and straw in small-scale combustion, Biomass Bioenergy 150 (2021) 106135, https://doi.org/10.1016/j.biombioe.2021.106135. S.
[11] R. Mack, D. Kuptz, C. Schön, H. Hartmann, Combustion behavior and slagging tendencies of kaolin additivated agricultural pellets and of wood-straw pellet blends in a small-scale boiler, Biomass Bioenergy 125 (2019) 50–62, https://doi.org/10.1016/j.biombioe.2019.04.003. S.
[12] B. Gudka, J.M. Jones, A.R. Lea-Langton, A. Williams, A. Saddawi, A review of the mitigation of deposition and emission problems during biomass combustion through washing pre-treatment, J. Energy Inst. 89 (2016) 159–171, https://doi.org/10.1016/j.joei.2015.02.007, 2, S.
[13] Commission Regulation (EU) 2015/1189 of 28 April 2015 Implementing Directive 2009/125/EC of the European Parliament and of the Council with Regard to Ecodesign Requirements for Solid Fuel Boilers.
[14] Y. Yang, V. Sharifi, J. Swithenbank, Effect of air flow rate and fuel moisture on the burning behaviours of biomass and simulated municipal solid wastes in packed beds, Fuel 83 (2004) 1553–1562, https://doi.org/10.1016/j.fuel.2004.01.016, 11-12, S.
[15] S. van Loo, J. Koppejan, The Handbook of Biomass Combustion and Co-firing, Earthscan, London, 2008.
[16] T. Nussbaumer, Combustion and Co-combustion of biomass: fundamentals, technologies, and primary measures for emission reduction, Energy Fuels 17 (6) (2003) 1510–1521, https://doi.org/10.1021/ef030031q. , S.
[17] B. Jenkins, Industrial and Process Furnaces - Principles, Design and Operation, third ed., Elsevier Science & Technology, San Diego, 2023.
[18] A. Boriouchkine, A. Zakharov, S.-L. Jämsä-Jounela, Dynamic modeling of combustion in a BioGrate furnace: the effect of operation parameters on biomass firing, Chem. Eng. Sci. 69 (2012) 669–678, https://doi.org/10.1016/j.ces.2011.11.032, 1, S.
[19] M. Kaltschmitt, H. Hartmann, H. Hofbauer, Energie aus Biomasse, Springer Berlin Heidelberg, Berlin, Heidelberg, 2016.
[20] M.T. Lim, A. Phan, D. Roddy, A. Harvey, Technologies for measurement and mitigation of particulate emissions from domestic combustion of biomass: a review, Renew. Sustain. Energy Rev. 49 (2015) 574–584, https://doi.org/10.1016/j.rser.2015.04.090. S.
[21] M.A. Ahmad Farid, M.A. Hassan, A.M. Roslan, M.H. Samsudin, Z.J.J. Mohamad, M.R. Othman, Y. Shirai, Carbon monoxide reduction in the flue gas during biochar production from oil palm empty fruit bunch, J. Clean. Prod. 258 (2020) 120580, https://doi.org/10.1016/j.jclepro.2020.120580. S.
[22] J. Akil, S. Siffert, P.-R. Laurence, D.P. Debecker, F. Devred, R. Cousin, C. Poupin, Effect of precious metals on NO reduction by CO in oxidative conditions, Appl. Sci. 10 (2020) 3042, https://doi.org/10.3390/app10093042, 9, S.
[23] T.S. Cam, T.A. Vishnievskaia, V.I. Popkov, Catalytic oxidation of CO over CuO/CeO 2 nanocomposites synthesized via solution combustion method: effect of fuels, Rev. Adv. Mater. Sci. 59 (2020) 131–143, https://doi.org/10.1515/rams-2020-0002, 1, S.
[24] D. Dakic, S. Belosevic, R. Mladenovic, M. Paprika, D. Djurovic, A. Eric, M. Komatina, B. Grbic, N. Radic, Reduction of carbon monoxide emission from a solid-fuel thermo-accumulation furnace, Therm. Sci. 10 (2006) 107–119, https://doi.org/10.2298/TSCI0604107D, 4, S.
[25] M. Ferrandon, M. Berg, E. Björnbom, Thermal stability of metal-supported catalysts for reduction of cold-start emissions in a wood-fired domestic boiler, Catal. Today 53 (4) (1999) 647–659, https://doi.org/10.1016/S0920-5861(99)00152-2. , S.
[26] F. Ozil, V. Tschamber, F. Haas, G. Trouvé, Efficiency of catalytic processes for the reduction of CO and VOC emissions from wood combustion in domestic fireplaces, Fuel Process. Technol. 90 (2009) 1053–1061, https://doi.org/10.1016/j.fuproc.2009.03.019, 9, S.
[27] R. Mack, C. Schön, D. Kuptz, H. Hartmann, T. Brunner, I. Obernberger, H.M. Behr, Influence of pellet length, content of fines, and moisture content on emission behavior of wood pellets in a residential pellet stove and pellet boiler, Biomass Conversion and Biorefinery (2022), https://doi.org/10.1007/s13399-022-03302-6.
[28] L. Lukáč, J. Kizek, G. Jablonský, Y. Karakash, Defining the mathematical dependencies of NO x and CO emission generation after biomass combustion in low-power boiler, civil and, Envir. Eng. Rep. 29 (2019) 153–163, https://doi.org/10.2478/ceer-2019-0031, 3, S.
[29] G. Schmidt, G. Trouvé, G. Leyssens, C. Schönnenbeck, P. Genevray, F. Cazier, D. Dewaele, C. Vandenbilcke, E. Faivre, Y. Denance, C. Le Dreff-Lorimier, Wood washing: influence on gaseous and particulate emissions during wood combustion in a domestic pellet stove, Fuel Process. Technol. 174 (2018) 104–117, https://doi.org/10.1016/j.fuproc.2018.02.020. S.
[30] F. Störner, F. Lind, M. Rydén, Oxygen carrier aided combustion in fluidized bed boilers in Sweden—review and future outlook with respect to affordable bed materials, Appl. Sci. 11 (2021) 7935, https://doi.org/10.3390/app11177935, 17, S.
[31] H. Khodaei, Y.M. Al-Abdeli, F. Guzzomi, G.H. Yeoh, An overview of processes and considerations in the modelling of fixed-bed biomass combustion, Energy 88 (2015) 946–972, https://doi.org/10.1016/j.energy.2015.05.099. S.
[32] T. Kaivosoja, A. Virén, J. Tissari, J. Ruuskanen, J. Tarhanen, O. Sippula, J. Jokiniemi, Effects of a catalytic converter on PCDD/F, chlorophenol and PAH emissions in residential wood combustion, Chemosphere 88 (2012) 278–285, https://doi.org/10.1016/j.chemosphere.2012.02.027, 3, S.
[33] M. Variny, A. Varga, M. Rimár, J. Janošovský, J. Kizek, L. Lukáč, G. Jablonský, O. Mierka, Advances in biomass Co-combustion with fossil fuels in the European context: a review, Processes 9 (2021) 100, https://doi.org/10.3390/pr9010100, 1, S.
[34] A. Zhou, H. Xu, M. Xu, W. Yu, Z. Li, W. Yang, Numerical investigation of biomass co-combustion with methane for NOx reduction, Energy 194 (2020), https://doi.org/10.1016/j.energy.2019.116868. S. 116868.
[35] A. Singhal, J. Konttinen, T. Joronen, Effect of different washing parameters on the fuel properties and elemental composition of wheat straw in water-washing pre-treatment. Part 1: effect of washing duration and biomass size, Fuel 292 (2021) 120206, https://doi.org/10.1016/j.fuel.2021.120206. S.
[36] P. Abelha, C. Mourão Vilela, P. Nanou, M. Carbo, A. Janssen, S. Leiser, Combustion improvements of upgraded biomass by washing and torrefaction, Fuel 253 (2019) 1018–1033, https://doi.org/10.1016/j.fuel.2019.05.050. S.
[37] J. Khalsa, F. Döhling, F. Berger, Foliage and grass as fuel pellets–small scale combustion of washed and mechanically leached biomass, Energies 9 (2016) 361, https://doi.org/10.3390/en9050361, 5, S.
[38] S.B. Liaw, H. Wu, Leaching characteristics of organic and inorganic matter from biomass by water: differences between batch and semi-continuous operations, Ind. Eng. Chem. Res. 52 (2013) 4280–4289, https://doi.org/10.1021/ie3031168, 11, S.
[39] J. Cai, S. Wang, C. Kuang, X. Tang, Insight into the kinetic analysis of catalytic combustion for biomass after alkaline metals loaded pretreatment, Fuel 203 (2017) 501–513, https://doi.org/10.1016/j.fuel.2017.04.137. S.

[40] D. Vamvuka, V. Tsamourgeli, M. Galetakis, Study on catalytic combustion of biomass mixtures with poor coals, Combust. Sci. Technol. 186 (2014) 68–82, https://doi.org/10.1080/00102202.2013.846331, 1, S.

[41] Yu Zhaosheng, Ma Xiaoqian, Liu Ao": Thermogravimetric Analysis of Rice and Wheat Straw Catalytic Combustion in Air- and Oxygen-Enriched Atmospheres.

[42] E.G. Pereira, H. Fauller, M. Magalhães, B. Guirardi, M.A. Martins, Potential use of wood pyrolysis coproducts: a review, Environ. Prog. Sustain. Energy 41 (2022), https://doi.org/10.1002/ep.13705.

[43] D. Chen, K. Cen, X. Zhuang, Z. Gan, J. Zhou, Y. Zhang, H. Zhang, Insight into biomass pyrolysis mechanism based on cellulose, hemicellulose, and lignin: evolution of volatiles and kinetics, elucidation of reaction pathways, and characterization of gas, biochar and bio-oil, Combust. Flame 242 (2022) 112142, https://doi.org/10.1016/j.combustflame.2022.112142. S.

[44] H. Yang, R. Yan, H. Chen, D.H. Lee, C. Zheng, Characteristics of hemicellulose, cellulose and lignin pyrolysis, Fuel 86 (2007) 1781–1788, https://doi.org/10.1016/j.fuel.2006.12.013, 12-13, S.

[45] P. Thanatawee, W. Rukthong, S. Sunphorka, P. Piumsomboon, B. Chalermsinsuwan, Effect of biomass compositions on combustion kinetic parameters using response surface methodology, Int. J. Chem. React. Eng. 14 (2016) 517–526, https://doi.org/10.1515/ijcre-2015-0082, 1, S.

[46] Y.B. Yang, V.N. Sharifi, J. Swithenbank, L. Ma, L.I. Darvell, J.M. Jones, M. Pourkashanian, A. Williams, Combustion of a single particle of biomass, Energy Fuels 22 (2008) 306–316, https://doi.org/10.1021/ef700305r, 1, S.

[47] Z. Liu, X. Ku, H. Jin, Pyrolysis mechanism of wheat straw based on ReaxFF molecular dynamics simulations, ACS Omega 7 (24) (2022) 21075–21085, https://doi.org/10.1021/acsomega.2c01899. , S.

[48] H. Hao, C.L. Chow, D. Lau, Carbon monoxide release mechanism in cellulose combustion using reactive forcefield, Fuel 269 (2020) 117422, https://doi.org/10.1016/j.fuel.2020.117422. S.

[49] Y. Su, Y. Luo, W. Wu, Y. Zhang, S. Zhao, Characteristics of pine wood oxidative pyrolysis: degradation behavior, carbon oxide production and heat properties, J. Anal. Appl. Pyrol. 98 (S) (2012) 137–143, https://doi.org/10.1016/j.jaap.2012.07.005.

[50] Y. Haseli, J.A. van Oijen, L.P.H. de Goey, A detailed one-dimensional model of combustion of a woody biomass particle, Bioresour. Technol. 102 (20) (2011) 9772–9782, https://doi.org/10.1016/j.biortech.2011.07.075. , S.

[51] K. Chenoweth, A.C.T. van Duin, W.A. Goddard, ReaxFF reactive force field for molecular dynamics simulations of hydrocarbon oxidation, J. Phys. Chem. A 112 (2008) 1040–1053, https://doi.org/10.1021/jp709896w, 5, S.

[52] A.C.T. van Duin, S. Dasgupta, F. Lorant, W.A. Goddard, ReaxFF: a reactive force field for hydrocarbons, J. Phys. Chem. 105 (2001) 9396–9409, https://doi.org/10.1021/jp004368u, 41, S.

[53] W. Guo, J. Wu, L. Meng, C. Geng, Y. Yang, N. Li, G. Wu, H. Zhang, Q. Guo, H. Bai, Reactive behaviors and mechanisms of cellulose in chemical looping combustions with iron-based oxygen carriers: an experimental combined with ReaxFF MD study, Applications in Energy and Combustion Science 14 (2023) 100135, https://doi.org/10.1016/j.jaecs.2023.100135. S.

[54] S. Bhoi, T. Banerjee, K. Mohanty, Molecular dynamic simulation of spontaneous combustion and pyrolysis of brown coal using ReaxFF, Fuel 136 (2014) 326–333, https://doi.org/10.1016/j.fuel.2014.07.058. S.

[55] F. Castro-Marcano, A.M. Kamat, M.F. Russo, A.C. van Duin, J.P. Mathews, Combustion of an Illinois No. 6 coal char simulated using an atomistic char representation and the ReaxFF reactive force field, Combust. Flame 159 (2012) 1272–1285, https://doi.org/10.1016/j.combustflame.2011.10.022, 3, S.

[56] B. Chen, Z. Diao, H. Lu, Using the ReaxFF reactive force field for molecular dynamics simulations of the spontaneous combustion of lignite with the Hatcher lignite model, Fuel 116 (2014) S. 7–13, https://doi.org/10.1016/j.fuel.2013.07.113.

[57] Dikun Hong, Liang Liu, Chunbo Wang, Ting Si, Xin Guo: Construction of a Coal Char Model and its Combustion and Gasification Characteristics: Molecular Dynamic Simulations Based on ReaxFF.

[58] C. Chen, L. Zhao, J. Wang, S. Lin, Reactive molecular dynamics simulations of biomass pyrolysis and combustion under various oxidative and humidity environments, Ind. Eng. Chem. Res. 56 (2017) 12276–12288, https://doi.org/10.1021/acs.iecr.7b01714, 43, S.

[59] E. Picheau, S. Amar, A. Derré, A. Pénicaud, F. Hof, An introduction to the combustion of carbon materials, Chemistry (Weinheim an der Bergstrasse, Germany) 28 (2022) e202200117, https://doi.org/10.1002/chem.202200117, 54, S.

[60] O. Karlström, L. Hupa, Energy conversion of biomass char: oxidation rates in mixtures of O2/CO2/H2O, Energy 181 (2019) 615–624, https://doi.org/10.1016/j.energy.2019.05.192. S.

[61] N.M. Laurendeau, Heterogeneous kinetics of coal char gasification and combustion, Prog. Energy Combust. Sci. 4 (1978) 221–270, https://doi.org/10.1016/0360-1285(78)90008-4, 4, S.

[62] K. Al-Qayim, W. Nimmo, K. Hughes, M. Pourkashanian, Kinetic parameters of the intrinsic reactivity of woody biomass and coal chars via thermogravimetric analysis, Fuel 210 (2017) 811–825, https://doi.org/10.1016/j.fuel.2017.09.010. S.

[63] D. Förtsch, R.H. Essenhigh, U. Schnell, K.R.G. Hein, On the application of the thiele/zeldovich analysis to porous carbon combustion, Energy Fuels 17 (4) (2003) 901–906, https://doi.org/10.1021/ef0202081. , S.

[64] C. Di Blasi, Combustion and gasification rates of lignocellulosic chars, Prog. Energy Combust. Sci. 35 (2009) 121–140, https://doi.org/10.1016/j.pecs.2008.08.001, 2, S.

[65] A.I. Bartlett, R.M. Hadden, L.A. Bisby, A review of factors affecting the burning behaviour of wood for application to tall timber construction, Fire Technol. 55 (2019) 1–49, https://doi.org/10.1007/s10694-018-0787-y, 1, S.

[66] I. Obernberger, Decentralised biomass combustion – state-of-the-art and future development, Copenhagen, Biomass Bioenergy 14 (1) (1996) 33–56. , S.

[67] S. Zhou, H. Su, Z. Wu, X. Zhu, B. Yan, G. Chen, Numerical study on self-ignition temperature of biomass gasified gas for the application of MILD combustion, Fuel Process. Technol. 236 (2022) 107417, https://doi.org/10.1016/j.fuproc.2022.107417. S.

[68] I. Haberle, Ø. Skreiberg, J. Łazar, N.E.L. Haugen, Numerical models for thermochemical degradation of thermally thick woody biomass, and their application in domestic wood heating appliances and grate furnaces, Prog. Energy Combust. Sci. 63 (S) (2017) 204–252, https://doi.org/10.1016/j.pecs.2017.07.004.

[69] A. Dhahak, R. Bounaceur, C. Le Dreff-Lorimier, G. Schmidt, G. Trouve, F. Battin-Leclerc, Development of a detailed kinetic model for the combustion of biomass, Fuel 242 (2019) 756–774, https://doi.org/10.1016/j.fuel.2019.01.093. S.

[70] E. Ranzi, M. Corbetta, F. Manenti, S. Pierucci, Kinetic modeling of the thermal degradation and combustion of biomass, Chem. Eng. Sci. 110 (2014) S. 2–12, https://doi.org/10.1016/j.ces.2013.08.014.

[71] P.E.A. Debiagi, G. Gentile, M. Pelucchi, A. Frassoldati, A. Cuoci, T. Faravelli, E. Ranzi, Detailed kinetic mechanism of gas-phase reactions of volatiles released from biomass pyrolysis, Biomass Bioenergy 93 (2016) 60–71, https://doi.org/10.1016/j.biombioe.2016.06.015. S.

[72] Xiaoyuan Zhang, S. Mani Sarathy: A Lumped Kinetic Model for High-Temperature Pyrolysis and Combustion of 50 Surrogate Fuel Components and Their Mixtures.

[73] M. Farokhi, M. Birouk, A new EDC approach for modeling turbulence/chemistry interaction of the gas-phase of biomass combustion, Fuel 220 (2018) 420–436, https://doi.org/10.1016/j.fuel.2018.01.125. S.

[74] A. Shiehnejadhesar, R. Mehrabian, R. Scharler, G.M. Goldin, I. Obernberger, Development of a gas phase combustion model suitable for low and high turbulence conditions, Fuel 126 (2014) 177–187, https://doi.org/10.1016/j.fuel.2014.02.040. S.

[75] J. Warnatz, The structure of laminar alkane-, alkene-, and acetylene flames, Symposium (International) on Combustion 18 (1981) 369–384, https://doi.org/10.1016/S0082-0784(81)80042-2, 1, S.

[76] H.-H. Carstensen, A.M. Dean, Development of Detailed Kinetic Models for the Thermal Conversion of Biomass via First Principle Methods and Rate Estimation Rules, 1052, 2010, pp. 201–243, https://doi.org/10.1021/bk-2010-1052.ch010. S.

[77] E. Ranzi, A. Frassoldati, A. Stagni, M. Pelucchi, A. Cuoci, T. Faravelli, Reduced kinetic schemes of complex reaction systems: fossil and biomass-derived transportation fuels, Int. J. Chem. Kinet. 46 (2014) 512–542, https://doi.org/10.1002/kin.20867, 9, S.

[78] J.B. Howard, G.C. Williams, D.H. Fine, Kinetics of carbon monoxide oxidation in postflame gases, Symposium (International) on Combustion 14 (1973) 975–986, https://doi.org/10.1016/S0082-0784(73)80089-X, 1, S.

[79] G. Dixon-Lewis, D.J. Williams, Chapter 1 the oxidation of hydrogen and carbon monoxide, in: Gas-phase Combustion, Elsevier, 1977.

[80] I. Glassman, R.A. Yetter, Combustion, fourth ed., Academic Press, Amsterdam, Boston, 2008.

[81] Wong, E. L., Potter, Jr. A. E., Belles, F. E.: Reaction Rates of Carbon Monoxide with Hydroxyl Radicals and Oxygen Atoms.

[82] H.-J. Freund, G. Meijer, M. Scheffler, R. Schlögl, M. Wolf, CO oxidation as a prototypical reaction for heterogeneous processes, Angew. Chem. 50 (2011) 10064–10094, https://doi.org/10.1002/anie.201101378, 43, S.

[83] S.R. Turns, An Introduction to Combustion - Concepts and Applications, McGraw-Hill series in mechanical engineering, McGraw-Hill, New York, 2012.

[84] J. Warnatz, Resolution of gas phase and surface combustion chemistry into elementary reactions, Symposium (International) on Combustion 24 (1992) 553–579, https://doi.org/10.1016/S0082-0784(06)80070-6, 1, S.

[85] A. Frassoldati, T. Faravelli, E. Ranzi, The ignition, combustion and flame structure of carbon monoxide/hydrogen mixtures. Note 1: detailed kinetic modeling of syngas combustion also in presence of nitrogen compounds, Int. J. Hydrogen Energy 32 (2007) 3471–3485, https://doi.org/10.1016/j.ijhydene.2007.01.011, 15, S.

[86] D.L. Baulch, C.T. Bowman, C.J. Cobos, R.A. Cox, T. Just, J.A. Kerr, M.J. Pilling, D. Stocker, J. Troe, W. Tsang, R.W. Walker, J. Warnatz, Evaluated kinetic data for combustion modeling: supplement II, J. Phys. Chem. Ref. Data 34 (2005) 757–1397, https://doi.org/10.1063/1.1748524, 3, S.

[87] G. von Elbe, B. Lewis, Free-radical reactions in glow and explosion of carbon monoxide–oxygen mixtures, Combust. Flame 63 (1986) 135–150, https://doi.org/10.1016/0010-2180(86)90116-1, 1-2, S.

[88] S.G. Davis, A.V. Joshi, H. Wang, F. Egolfopoulos, An optimized kinetic model of H2/CO combustion, Proc. Combust. Inst. 30 (2005) 1283–1292, https://doi.org/10.1016/j.proci.2004.08.252, 1, S.

[89] P. Gray, J.F. Griffiths, S.K. Scott, Oscillations, glow and ignition in carbon monoxide oxidation in an open system. I. Experimental studies of the ignition diagram and the effects of added hydrogen, Proceed. Royal Soc. London. A. Mathemat. Phy. Sci. 397 (1985) 21–44, https://doi.org/10.1098/rspa.1985.0002, 1812, S.

[90] Wenkai Liang and Chung K. Law: on Radical-Induced Ignition in Combustion Systems.

[91] C. Ryu, Y.B. Yang, A. Khor, N.E. Yates, V.N. Sharifi, J. Swithenbank, Effect of fuel properties on biomass combustion: Part I. Experiments—fuel type, equivalence

ratio and particle size, Fuel 85 (2006) 1039–1046, https://doi.org/10.1016/j.fuel.2005.09.019, 7-8, S.

[92] M. Abián, J. Giménez-López, R. Bilbao, M.U. Alzueta, Effect of different concentration levels of CO2 and H2O on the oxidation of CO: experiments and modeling, Proc. Combust. Inst. 33 (2011) 317–323, https://doi.org/10.1016/j.proci.2010.05.078, 1, S.

[93] J. Yu, Q. Guo, Y. Gong, L. Ding, J. Wang, G. Yu, A review of the effects of alkali and alkaline earth metal species on biomass gasification, Fuel Process. Technol. 214 (2021), https://doi.org/10.1016/j.fuproc.2021.106723. S. 106723.

[94] P. Glarborg, Hidden interactions—trace species governing combustion and emissions, Proc. Combust. Inst. 31 (2007) 77–98, https://doi.org/10.1016/j.proci.2006.08.119, 1, S.

[95] German version EN 16510-1:2022, Residential Solid Fuel Burning Appliances – Part 1: General Requirements and Test Methods, 2023.

[96] F. Endriss, P. Grammer, M. Russ, H. Thorwarth, Impact of chimney-draught conditions on combustion and emission behavior of a wood-burning stove, Chem. Ing. Tech. 93 (2021) 412–420, https://doi.org/10.1002/cite.202000098, 3, S.

[97] Robert Mack, TFZ-Bericht 57: Optimierungspotenziale bei Kaminöfen –Emissionen, Wirkungsgrad und Wärmeverluste, Stand, August 2018.

[98] A. Doberer, J. Good, T. Nussbaumer, PARTIKELEMISSIONEN VON HOLZFEUERUNGEN BIS 70 KW: - Betriebseinfluss auf die Feinstaubemissionen von Holzfeuerungen, 2009.

[99] G. Reichert, H. Hartmann, W. Haslinger, H. Oehler, R. Mack, C. Schmidl, C. Schön, M. Schwabl, H. Stressler, R. Sturmlechner, C. Hochenauer, Effect of draught conditions and ignition technique on combustion performance of firewood roomheaters, Renew. Energy 105 (2017) 547–560, https://doi.org/10.1016/j.renene.2016.12.017. S.

[100] M. Struschka, M.D. Carrasco Martín, G. Baumbach, Durchführung von Feldmessungen an Feuerungsanlagen mit Sensoren, 2009.

[101] M. Sami, K. Annamalai, M. Wooldridge, Co-firing of coal and biomass fuel blends, Prog. Energy Combust. Sci. 27 (2001) 171–214, https://doi.org/10.1016/S0360-1285(00)00020-4, 2, S.

[102] Qurat ul-Ain, M. Shafiq, S.C. Capareda, Firdaus-e-Bareen: effect of different temperatures on the properties of pyrolysis products of Parthenium hysterophorus, J. Saudi Chem. Soc. 25 (2021) 101197, https://doi.org/10.1016/j.jscs.2021.101197, 3, S.

[103] A. Selvarajoo, D. Oochit, Effect of pyrolysis temperature on product yields of palm fibre and its biochar characteristics, Mater. Sci. Energy Technol. 3 (2020) 575–583, https://doi.org/10.1016/j.mset.2020.06.003. S.

[104] P. Mathieu, R. Dubuisson, Performance analysis of a biomass gasifier, Energy Convers. Manag. 43 (2002) 1291–1299, https://doi.org/10.1016/S0196-8904(02)00015-8, 9-12, S.

[105] A. Chanpirak, H. Hashemi, F.J. Frandsen, H. Wu, P. Glarborg, P. Marshall, The chemical coupling between moist CO oxidation and gas-phase potassium sulfation, Fuel 336 (2023) 127127, https://doi.org/10.1016/j.fuel.2022.127127. S.

[106] J. Wei, M. Wang, D. Xu, L. Shi, B. Li, Y. Bai, G. Yu, W. Bao, J. Xu, H. Zhang, S. Zhang, Migration and transformation of alkali/alkaline earth metal species during biomass and coal co-gasification: a review, Fuel Process. Technol. 235 (2022) 107376, https://doi.org/10.1016/j.fuproc.2022.107376. S.

[107] H. Zhu, Q. Liao, L. Hu, L. Xie, B. Qu, R. Gao, Effect of removal of alkali and alkaline earth metals in cornstalk on slagging/fouling and co-combustion characteristics of cornstalk/coal blends for biomass applications, Renew. Energy 207 (2023) 275–285, https://doi.org/10.1016/j.renene.2023.03.022. S.

[108] W. Cheng, Y. Zhu, J. Shao, W. Zhang, G. Wu, H. Jiang, J. Hu, Z. Huang, H. Yang, H. Chen, Mitigation of ultrafine particulate matter emission from agricultural biomass pellet combustion by the additive of phosphoric acid modified kaolin, Renew. Energy 172 (2021) 177–187, https://doi.org/10.1016/j.renene.2021.03.041. S.

[109] J.L. Míguez, J. Porteiro, F. Behrendt, D. Blanco, D. Patiño, A. Dieguez-Alonso, Review of the use of additives to mitigate operational problems associated with the combustion of biomass with high content in ash-forming species, Renew. Sustain. Energy Rev. 141 (2021) 110502, https://doi.org/10.1016/j.rser.2020.110502. S.

[110] P. Giudicianni, V. Gargiulo, C.M. Grottola, M. Alfè, A.I. Ferreiro, M.A.A. Mendes, M. Fagnano, R. Ragucci, Inherent metal elements in biomass pyrolysis: a review, Energy Fuels 35 (2021) 5407–5478, https://doi.org/10.1021/acs.energyfuels.0c04046, 7, S.

[111] J.G. Olsson, U. Jäglid, J.B.C. Pettersson, P. Hald, Alkali metal emission during pyrolysis of biomass, Energy Fuels 11 (1997) 779–784, https://doi.org/10.1021/ef960096b, 4, S.

[112] Z. Zhang, J. Liu, F. Shen, Y. Dong, Insights into the effects of atmosphere and chlorine on potassium release during biomass combustion: temporal measurement and kinetic studies, Energy Fuels 32 (2018) 12523–12531, https://doi.org/10.1021/acs.energyfuels.8b02399, 12, S.

[113] J.M. Johansen, J.G. Jakobsen, F.J. Frandsen, P. Glarborg, Release of K, Cl, and S during pyrolysis and combustion of high-chlorine biomass, Energy Fuels 25 (11) (2011) 4961–4971, https://doi.org/10.1021/ef201098n. , S.

[114] A. Saddawi, J.M. Jones, A. Williams, Influence of alkali metals on the kinetics of the thermal decomposition of biomass, Fuel Process. Technol. 104 (2012) 189–197, https://doi.org/10.1016/j.fuproc.2012.05.014. S.

[115] L. Ma, J.M. Jones, M. Pourkashanian, A. Williams, Modelling the combustion of pulverized biomass in an industrial combustion test furnace, Fuel 86 (2007) 12–13, https://doi.org/10.1016/j.fuel.2006.12.019. , S. 1959–1965.

[116] R. Fahmi, A.V. Bridgwater, L.I. Darvell, J.M. Jones, N. Yates, S. Thain, I. S. Donnison, The effect of alkali metals on combustion and pyrolysis of Lolium and Festuca grasses, switchgrass and willow, Fuel 86 (2007) 1560–1569, https://doi.org/10.1016/j.fuel.2006.11.030, 10-11, S.

[117] J.M. Jones, L.I. Darvell, M. Pourkashanian, A. Williams, The role of metals in biomass char combustion, in: Proceedings of the European Combustion Meeting, 2005.

[118] S. Hu, L. Jiang, Y. Wang, S. Su, L. Sun, B. Xu, L. He, J. Xiang, Effects of inherent alkali and alkaline earth metallic species on biomass pyrolysis at different temperatures, Bioresour. Technol. 192 (2015) 23–30, https://doi.org/10.1016/j.biortech.2015.05.042. S.

[119] A. Demirbaş, Gaseous products from biomass by pyrolysis and gasification: effects of catalyst on hydrogen yield, Energy Convers. Manag. 43 (2002) 897–909, https://doi.org/10.1016/S0196-8904(01)00080-2, 7, S.

[120] L. Devi, K.J. Ptasinski, F.J. Janssen, A review of the primary measures for tar elimination in biomass gasification processes, Biomass Bioenergy 24 (2003) 125–140, https://doi.org/10.1016/S0961-9534(02)00102-2, 2, S.

[121] T. Dahou, F. Defoort, B. Khiari, M. Labaki, C. Dupont, M. Jeguirim, Role of inorganics on the biomass char gasification reactivity: a review involving reaction mechanisms and kinetics models, Renew. Sustain. Energy Rev. 135 (2021) 110136, https://doi.org/10.1016/j.rser.2020.110136. S.

[122] L. Jiang, S. Hu, Y. Wang, S. Su, L. Sun, B. Xu, L. He, J. Xiang, Catalytic effects of inherent alkali and alkaline earth metallic species on steam gasification of biomass, Int. J. Hydrogen Energy 40 (2015) 15460–15469, https://doi.org/10.1016/j.ijhydene.2015.08.111, 45, S.

[123] C. Du, L. Liu, P. Qiu, Importance of volatile AAEM species to char reactivity during volatile–char interactions, RSC Adv. 7 (2017) 10397–10406, https://doi.org/10.1039/C6RA27485D, 17, S.

[124] T. Berdugo Vilches, W. Weng, P. Glarborg, Z. Li, H. Thunman, M. Seemann, Shedding light on the governing mechanisms for insufficient CO and H2 burnout in the presence of potassium, chlorine and sulfur, Fuel 273 (2020) 117762, https://doi.org/10.1016/j.fuel.2020.117762. S.

[125] S.C. van Lith, V. Alonso-Ramírez, P.A. Jensen, F.J. Frandsen, P. Glarborg, Release to the gas phase of inorganic elements during wood combustion. Part 1: development and evaluation of quantification methods, Energy Fuels 20 (3) (2006) 964–978, https://doi.org/10.1021/ef050131r. , S.

[126] S.C. van Lith, P.A. Jensen, F.J. Frandsen, P. Glarborg, Release to the gas phase of inorganic elements during wood combustion. Part 2: influence of fuel composition, Energy Fuels 22 (2008) 1598–1609, https://doi.org/10.1021/ef060613i, 3, S.

[127] P. Glarborg, D. Kubel, K. Dam-Johansen, H.-M. Chiang, J.W. Bozzelli, Impact of SO2 and NO on CO oxidation under post-flame conditions, Int. J. Chem. Kinet. 28 (1996) 773–790, https://doi.org/10.1002/(SICI)1097-4601(1996)28:10<773:AID-KIN8>3.0.CO;2-K, 10, S.

[128] P. Glarborg, D. Kubel, P.G. Kristensen, J. Hansen, K. Dam-Johansen, Interactions of CO, NO x and H 2 O under post-flame conditions, Combust. Sci. Technol. 110–111 (1) (1995) 461–485, https://doi.org/10.1080/00102209508951936. , S.

[129] A. Chanpirak, H. Wu, P. Glarborg, P. Marshall, An experimental and chemical kinetic modeling study of the role of potassium in the moist oxidation of CO, Fuel 335 (2023) 127075, https://doi.org/10.1016/j.fuel.2022.127075. S.

[130] T. Brunner, I. Obernberger, Advanced Characterisation Methods for Solid Biomass Fuels, 32, IEA Bioenergy Task, 2015.

[131] L.S. Johansson, C. Tullin, B. Leckner, P. Sjövall, Particle emissions from biomass combustion in small combustors, Biomass Bioenergy 25 (2003) 435–446, https://doi.org/10.1016/S0961-9534(03)00036-9, 4, S.

[132] L. Rodríguez-Machín, R. Piloto-Rodríguez, A. Rubio-González, P.J. Iturria-Quintero, F. Ronsse, Pretreatment of sugarcane residues for combustion in biomass power stations: a review, Sugar Tech 24 (2022) 732–745, https://doi.org/10.1007/s12355-021-01091-2, 3, S.

[133] H. Cui, S.Q. Turn, T. Tran, D. Rogers, Mechanical dewatering and water leaching pretreatment of fresh banagrass, Guinea grass, energy cane, and sugar cane: characterization of fuel properties and byproduct streams, Fuel Process. Technol. 139 (2015) 159–172, https://doi.org/10.1016/j.fuproc.2015.07.027. S.

[134] K.O. Davidsson, J.G. Korsgren, J. Pettersson, U. Jäglid, The effects of fuel washing techniques on alkali release from biomass, Fuel 81 (2) (2002) 137–142, https://doi.org/10.1016/S0016-2361(01)00132-6. , S.

[135] S. Arvelakisa, P. Vourliotisb, E. Kakarasb, E.G. Koukiosa, Effect of leaching on the ash behavior of wheat straw and olive residue during fluidized bed combustion, Fuel Energy Abstr. 43 (2002) 206, https://doi.org/10.1016/S0140-6701(02)85900-8, 3, S.

[136] H. Beidaghy Dizaji, T. Zeng, I. Hartmann, D. Enke, T. Schliermann, V. Lenz, M. Bidabadi, Generation of high quality biogenic silica by combustion of rice husk and rice straw combined with pre- and post-treatment strategies—a review, Appl. Sci. 9 (2019) 1083, https://doi.org/10.3390/app9061083, 6, S.

[137] D.C. Dayton, B.M. Jenkins, S.Q. Turn, R.R. Bakker, R.B. Williams, D. Belle-Oudry, L.M. Hill, Release of inorganic constituents from leached biomass during thermal conversion, Energy Fuels 13 (1999) 860–870, https://doi.org/10.1021/ef980256e, 4, S.

[138] P. Ravichandran, K. Corscadden, Comparison of gaseous and particle emissions produced from leached and un-leached agricultural biomass briquettes, Fuel Process. Technol. 128 (2014) 359–366, https://doi.org/10.1016/j.fuproc.2014.07.030. S.

[139] M. Nishimura, S. Iwasaki, M. Horio, The role of potassium carbonate on cellulose pyrolysis, J. Taiwan Inst. Chem. Eng. 40 (2009) 630–637, https://doi.org/10.1016/j.jtice.2009.05.005, 6, S.

[140] D. Vamvuka, V. Tsamourgeli, M. Galetakis, Study on catalytic combustion of biomass mixtures with poor coals, Combust. Sci. Technol. 186 (2014) 68–82, https://doi.org/10.1080/00102202.2013.846331, 1, S.
[141] L. Wang, Y. Guo, Y. Zhu, Y. Qu, Y. Li, C. Rong, Z. Wang, Y. Liu, Investigation on catalyzed combustion of wheat straw by thermal analysis, Thermochim. Acta 512 (2011) 254–257, https://doi.org/10.1016/j.tca.2010.11.006, 1-2, S.
[142] M.J. San José, S. Alvarez, R. López, Catalytic combustion of vineyard pruning waste in a conical spouted bed combustor, Catal. Today 305 (2018) 13–18, https://doi.org/10.1016/j.cattod.2017.11.020. S.
[143] J. Cai, S. Wang, C. Kuang, X. Tang, Insight into the kinetic analysis of catalytic combustion for biomass after alkaline metals loaded pretreatment, Fuel 203 (2017) 501–513, https://doi.org/10.1016/j.fuel.2017.04.137. S.
[144] K. Le Manquais, C. Snape, J. Barker, I. McRobbie, TGA and drop tube furnace investigation of alkali and alkaline earth metal compounds as coal combustion additives, Energy Fuels 26 (3) (2012) 1531–1539, https://doi.org/10.1021/ef201936g. , S.
[145] Y. Zhaosheng, M. Xiaoqian, L. Ao, Kinetic studies on catalytic combustion of rice and wheat straw under air- and oxygen-enriched atmospheres, by using thermogravimetric analysis, Biomass Bioenergy 32 (2008) 1046–1055, https://doi.org/10.1016/j.biombioe.2008.02.001, 11, S.
[146] Y. Zhaosheng, M. Xiaoqian, L. Ao, Thermogravimetric analysis of rice and wheat straw catalytic combustion in air- and oxygen-enriched atmospheres, Energy Convers. Manag. 50 (2009) 561–566, https://doi.org/10.1016/j.enconman.2008.10.022, 3, S.
[147] L. Wang, J.E. Hustad, Ø. Skreiberg, G. Skjevrak, M. Grønli, A critical review on additives to reduce ash related operation problems in biomass combustion applications, Energy Proc. 20 (2012) 20–29, https://doi.org/10.1016/j.egypro.2012.03.004. S.
[148] J.L. Míguez, J. Porteiro, F. Behrendt, D. Blanco, D. Patiño, A. Dieguez-Alonso, Review of the use of additives to mitigate operational problems associated with the combustion of biomass with high content in ash-forming species, Renew. Sustain. Energy Rev. 141 (2021) 110502, https://doi.org/10.1016/j.rser.2020.110502. S.
[149] R. Mack, C. Schön, D. Kuptz, H. Hartmann, T. Brunner, I. Obernberger, H.M. Behr, Influence of wood species and additives on emission behavior of wood pellets in a residential pellet stove and a boiler, Biomass Conversion and Biorefinery (2023), https://doi.org/10.1007/s13399-023-04204-x.
[150] S. Ozgen, Methods for particulate matter emission reduction from pellet boilers, Biomass Conversion and Biorefinery (2022), https://doi.org/10.1007/s13399-022-03045-4.
[151] L.S. Bäfver, M. Rönnbäck, B. Leckner, F. Claesson, C. Tullin, Particle emission from combustion of oat grain and its potential reduction by addition of limestone or kaolin, Fuel Process. Technol. 90 (2009) 353–359, https://doi.org/10.1016/j.fuproc.2008.10.006, 3, S.
[152] M. Gehrig, M. Wöhler, S. Pelz, J. Steinbrink, H. Thorwarth, Kaolin as additive in wood pellet combustion with several mixtures of spruce and short-rotation-coppice willow and its influence on emissions and ashes, Fuel 235 (2019) 610–616, https://doi.org/10.1016/j.fuel.2018.08.028. S.
[153] A. Rebbling, J. Fagerström, E. Steinvall, M. Carlborg, M. Öhman, C. Boman, Reduction of alkali release by two fuel additives at different bed temperatures during grate combustion of woody biomass, Energy Fuels 33 (2019) 11041–11048, https://doi.org/10.1021/acs.energyfuels.9b02391, 11, S.
[154] Y. Niu, Y. Lv, X. Zhang, D. Wang, P. Li, S. Hui, Effects of water leaching (simulated rainfall) and additives (KOH, KCl, and SiO2) on the ash fusion characteristics of corn straw, Appl. Therm. Eng. 154 (S) (2019) 485–492, https://doi.org/10.1016/j.applthermaleng.2019.03.124.
[155] I. Höfer, M. Kaltschmitt, Effect of additives on particulate matter formation of solid biofuel blends from wood and straw, Biomass Conversion and Biorefinery 7 (2017) 101–116, https://doi.org/10.1007/s13399-016-0217-7, 1, S.
[156] S. Xiong, J. Burvall, H. Örberg, G. Kalen, M. Thyrel, M. Öhman, D. Boström, Slagging characteristics during combustion of corn stovers with and without kaolin and calcite, Energy Fuels 22 (5) (2008) 3465–3470, https://doi.org/10.1021/ef700718j. , S.
[157] T. Siegmund, C. Gollmer, M. Kaltschmitt, Carbon monoxide (CO) and particulate matter (PM) emissions during the combustion of wood pellets in a small-scale combustion unit – influence of aluminum-(silicate-)based fuel additivation, Fuel Process. Technol. (2024), https://doi.org/10.1016/j.fuproc.2024.108111.
[158] J. Marinkovic, H. Thunman, P. Knutsson, M. Seemann, Characteristics of olivine as a bed material in an indirect biomass gasifier, Chem. Eng. J. 279 (2015) 555–566, https://doi.org/10.1016/j.cej.2015.05.061. S.
[159] M. Rydén, M. Hanning, F. Lind, Oxygen carrier aided combustion (OCAC) of wood chips in a 12 MWth circulating fluidized bed boiler using steel converter slag as bed material, Appl. Sci. 8 (2018) 2657, https://doi.org/10.3390/app8122657, 12, S.
[160] F. Hildor, T. Mattisson, H. Leion, C. Linderholm, M. Rydén, Steel converter slag as an oxygen carrier in a 12 MWth CFB boiler – ash interaction and material evolution, Int. J. Greenh. Gas Control 88 (2019) 321–331, https://doi.org/10.1016/j.ijggc.2019.06.019. S.
[161] J. Marinkovic, H. Thunman, P. Knutsson, M. Seemann, Characteristics of olivine as a bed material in an indirect biomass gasifier, Chem. Eng. J. 279 (2015) 555–566, https://doi.org/10.1016/j.cej.2015.05.061. S.
[162] A. Larsson, M. Seemann, D. Neves, H. Thunman, Evaluation of performance of industrial-scale dual fluidized bed gasifiers using the chalmers 2–4-MW th gasifier, Energy Fuels 27 (2013) 6665–6680, https://doi.org/10.1021/ef400981j, 11, S.
[163] H. Thunman, M. Seemann, T. Berdugo Vilches, J. Maric, D. Pallares, H. Ström, G. Berndes, P. Knutsson, A. Larsson, C. Breitholtz, O. Santos, Advanced biofuel production via gasification – lessons learned from 200 man-years of research activity with Chalmers' research gasifier and the GoBiGas demonstration plant, Energy Sci. Eng. 6 (2018) 6–34, https://doi.org/10.1002/ese3.188, 1.
[164] H. Kassman, J. Pettersson, B.-M. Steenari, L.-E. Åmand, Two strategies to reduce gaseous KCl and chlorine in deposits during biomass combustion — injection of ammonium sulphate and co-combustion with peat, Fuel Process. Technol. 105 (2013) 170–180, https://doi.org/10.1016/j.fuproc.2011.06.025. S.
[165] H. Kassman, L. Bäfver, L.-E. Åmand, The importance of SO2 and SO3 for sulphation of gaseous KCl – an experimental investigation in a biomass fired CFB boiler, Combust. Flame 157 (2010) 1649–1657, https://doi.org/10.1016/j.combustflame.2010.05.012, 9, S.